A Novel Hybrid Drug between Two Potent Anti-tubulin Agents as a Potential Prolonged Anticancer Approach

Journal:	*Molecular Pharmaceutics*
Manuscript ID:	Draft
Manuscript Type:	Article
Date Submitted by the Author:	n/a
Complete List of Authors:	Marchetti, Paolo; University of Ferrara, Department of Chemical and Pharmaceutical Sciences Pavan, Barbara; University of Ferrara, Department of Life Sciences and Biotechnology Simoni, Daniele; University of Ferrara, Department of Chemical and Pharmaceutical Sciences Baruchello, Riccardo; University of Ferrara, Department of Chemical and Pharmaceutical Sciences Rondanin, Riccardo; University of Ferrara, Department of Chemical and Pharmaceutical Sciences Mischiati, Carlo; University of Ferrara, Department of Biomedical Sciences and Surgical Specialist Feriotto, Giordana; University of Ferrara, Department of Morphology, Surgery and Experimental Medicine Ferraro, Luca; University of Ferrara, Department of Life Sciences and Biotechnology Hsu, Lih-Ching; National Taiwan University, 1School of Pharmacy, College of Medicine Lee, Ray; Lestoni Corporation., Dalpiaz, Alessandro; University of Ferrara, Department of Chemical and Pharmaceutical Sciences

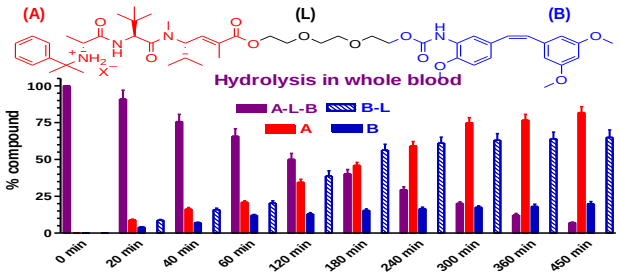
(A)
(L)
(B)
Hydrolysis in whole blood
A-L-B
B-L
A
B
% compound
100
75
50
25
0
0 min
20 min
40 min
60 min
120 min
180 min
240 min
300 min
360 min
450 min

A Novel Hybrid Drug between Two Potent Anti-tubulin Agents as a Potential Prolonged Anticancer Approach

Paolo Marchetti,[†] Barbara Pavan,[‡] Daniele Simoni,[†] Riccardo Baruchello,[†] Riccardo Rondanin,[†] Carlo Mischiati,[#] Giordana Feriotto,[§] Luca Ferraro,[‡] Lih-Ching Hsu[⌉], Ray M. Lee[⌋], Alessandro Dalpiaz*[,†]

[†]Department of Chemical and Pharmaceutical Sciences,[‡]Department of Life Sciences and Biotechnology, [#]Department of Biomedical Sciences and Surgical Specialist, [§]Department of Morphology, Surgery and Experimental Medicine, University of Ferrara, Ferrara, Italy.

[⌉]School of Pharmacy, College of Medicine, National Taiwan University, Taipei, Taiwan.

[⌋]Lestoni Corp., Richmond, VA, USA

ABSTRACT. Overcoming the toxicity and resistance associated with anti-cancer drugs is essential to the development of next generation therapy. An interesting approach is to combine two or more active components into a hybrid molecule. Here we report the design and synthesis of a novel hybrid drug by conjugation of two tubulin inhibitors, a hemiasterlin derivative ***A*** and a stilbene-based combretastatin analog ***B*** with a triethylene glycol linker (***L***) by ester and carbamate bonds, respectively. Biological activities such as the inhibitory activity against SKOV3 ovarian cancer cell growth were analyzed. The rationale is based on our recent finding of synergism between these two potent anti-microtubule agents ***A*** and ***B***. The IC_{50} values obtained in SKOV3 cells were 7.48 ± 1.27 nM for ***A***, 40.3 ± 6.28nM for ***B***, 738 ± 38.5 nM for ***A-L*** and 37.9 ± 2.11 nM for ***A-L-B***. ***A-L*** was much less potent compared to ***A***, and so was ***B-L*** compared to ***B***. A synergism between ***A*** and ***B*** was evidenced also in their conjugate form. HPLC analysis showed that in rat whole blood the hybrid ***A-L-B*** undergo hydrolysis of the ester bond between ***A*** and ***L*** (half-life = 118.2 ± 9.5 min) but not the carbamate bond between **B** and **L**; the hydrolysis product ***B-L*** was further hydrolyzed, but with a slower rate (half-life = 288 ± 12 min). The compound ***A-L*** was the faster hydrolyzed conjugate (half-life = 25.4±1.1 min). Taken together, these results suggest that the hybrid molecule ***A-L-B*** can release the potent anticancer ***A*** in biological settings. We have demonstrated the ability of this drug to elude the action of multidrug resistance P-gp channel, as shown by the permeation experiments across human colonic epithelial NCM460 cell monolayers. The poor ***A-L-B*** water solubility (0.015 ± 0.001 mg/ml) suggests its suitably to be encapsulated in nanoparticulate systems for selectively targeting tumor tissues.

KEYWORDS: *hemiasterlin, stilbene, hybrid drug, HPLC, rat blood, hydrolysis, permeation, SKOV3cell line, NCM460 cell line.*

INTRODUCTION

Microtubules of the cytoskeleton are composed of α- and β-tubulin heterodimers[1] and are highly dynamic structures, undergoing cycles of polymerization and depolymerization. These microtubule dynamics are essential for the maintenance and regulation of cell division.[2,3] Molecules perturbing the microtubule dynamics can be employed as effective anticancer drugs,[3,4] to induce apoptosis and to inhibit cell proliferation.[5]

Several tubulin binding sites have been identified for specific families of agents characterized by anti-microtubule activity: (*i*) the binding site for *vinka alkaloids* on β-tubulin; (*ii*) the c*olchicine* binding site located in the interface between α and β subunits of the tubulin dimer and (*iii*) the *taxane* binding site in the NH_2 terminal aminoacids of β-tubulin.[5]

Vinca alkaloids induce tubulin depolymerization; among these vincristine and vinblastine are approved for clinical use, whereas the semisynthetic agent vinflunine is in clinical trials. However, *vinca alkaloids* are subjected to the multidrug resistance (MDR) phenomenon, which is mediated by the active ABC efflux transporter P-glycoprotein (P-gp).[5,6]

Colchicine is a natural alkaloid that induces microtubule depolymerization, but it causes severe toxicity at the doses required for anticancer effects.[5] Stilbene derivatives such as the natural *cis*-stilbene combretastatin A-4 (CA-4) show an exceptionally strong tubulin inhibitory activity by acting at the colchicine binding site of tubulin.[7] Interestingly, CA-4 is not recognized by the ABC active efflux transporters, and not subject to the MDR phenomenon.[5] Recently, several active stilbenes were identified such as *cis*-3,4',5-trimethoxy-3'aminostilbene (Figure 1, compound ***B***), which induces apoptosis in HL60 leukemia cells at nanomolar concentrations.[8]

Taxanes, such as paclitaxel and docetaxel, have anticancer activity by stabilization of the microtubules. However, their clinical use has been limited by drug resistance, a multifactorial

phenomenon involving the overexpression of the active efflux transporter P-gp on the membrane of cancer cells.[5]

The hemiasterlins constitute a family of natural tripeptides, discovered from marine sponges, able to inhibit tubulin polymerization.[5,9-11] The tubuline binding site of this class of compounds is hypothesized near to that of *vinca alkaloids*, whose activity is non-competitively inhibited by hemiasterlins.[9] Taltobulin is a synthetic analogue of hemiasterlins showing improved *in vivo* cytotoxicity in comparison with vincristine and paclitaxel.[12] Interestingly, taltobulin is able to circumvent P-gp mediated resistance *in vitro* and *in vivo*.[10] The taltobulin synthesis was achieved by condensation of three non-natural amino acids; however, the enantioselective synthesis of one of these amino acids was very difficult.[11,13] Recently, a versatile enantioselective approach to a new class of synthetic hemiasterlins has been proposed.[13] The new hemiasterlins (Figure 1) proved as potent tubulin inhibitors and were able to induce a strong synergism with *cis*-3,4',5-trimethoxy-3'aminostilbene (compound ***B***, Figure 1).[14]

Taking into account all these aspects, it was interesting to investigate on new tubulin agents obtained by the conjugation of the compounds ***A*** and ***B***. This paper reports the synthesis and characterization of the hybrid compound obtained by coupling the hemiasterlin ***A*** and stilbene ***B*** derivatives using triethylenglicole (***L***) as a spacer (compound ***A-L-B***, Figure 1). We studied the hybrid compound in its cytotoxic activity and its potential hydrolysis in physiologic fluids (such as cell culture media, whole blood and liver homogenates) in order to investigate the potential ability of this conjugate to release the active components ***A*** and ***B***. To achieve this aim, we developed an efficacious analytical method via HPLC-UV for quantifying the hybrid compound ***A-L-B*** and its potential hydrolysis products ***A***, ***A-L***, ***B*** and ***B-L*** in all incubation media (Figure 1). The synthesis and the cytotoxic activities of the compounds ***A***, ***B*** and ***B-L*** have been reported previously.[8,13-15] We completed a series of potential hydrolysis products of the hybrid ***A-L-B*** along with the synthesis of compound ***A-L***, to characterize its cytotoxicity. The potential hydrolysis of the compounds ***A-L*** and ***B-L*** was also analyzed. Finally, monolayers of human normal colonic

epithelial cells have been validated as an *in vitro* model for evaluating the potential ability of the hemiasterlin derivative ***A*** (the main active hydrolysis product of the hybrid ***A-L-B***) to elude the P-pg efflux transporters.

MATERIALS AND METHODS

Chemistry. Commercially available solvents and reagents were used without further purification. Reactions and product mixtures were routinely monitored by thin-layer chromatography (TLC) on silica gel precoated plates (Merck F254) using the indicated solvent systems. Flash chromatography was carried out with Merck silica gel (230-400 mesh). All the final products undergoing biological testing were purified by preparative reversed phase HPLC [Waters Delta Prep LC 40 mm assembly column C18 (30 cm x 4 cm, 15 μm particle size)] eluted at a flow rate of 20 mL/min with mobile phase solvent A (10% CH_3CN + 0.1 % TFA in H_2O v/v), and a linear gradient from 10% to 60% B (60% CH_3CN + 0.1 % TFA in H_2O v/v) in 25 min. Melting points were determined on a Reichert-Kofler apparatus and are uncorrected. NMR spectra (^1H and ^{13}C) were recorded on a Varian-Mercury Plus 400 spectrometer and chemical shifts are given in parts per million (δ) downfield from tetramethylsilane (TMS) as an internal standard; *J* values are expressed in Hz. Molecular weights of compounds were determined by a mass spectrometer ESIMicromass ZMD-2000, values are expressed as MH^+. Light petroleum (PE) refers to the fractions boiling in the range 40-60 °C. All drying operations were performed over anhydrous sodium sulfate and evaporated with a rotatory evaporator. The purity of tested compounds was determined by combustion elemental analyses conducted by the Microanalytical Laboratory of the Pharmaceutical and Chemistry Department of the University of Ferrara with a Yanagimoto MT-5 CHN recorder elemental analyzer. All tested compounds yielded data within ± 0.4% of calculated values.

The hemiasterlin derivative ***A*** (Figure 1), the compounds *cis-3,4',5-trimethoxy-3'-aminostilbene, hydrochloride* (***B***, Figure 1), *cis-3,4',5-trimethoxy-3'carbamic acid 2-[2-(2-hydroxyethoxy)ethoxy]ethylesterstilbene* (***B-L***, Figure 1) and *cis-3,4',5-trimethoxy-3'-hydroxystilbene* (***C***, Figure 1) were synthetized as previously described.[13,15]

*Compound **A-L***. A solution of TEG (76.6 mg, 0.51 mmol) and DIEA (26.3 mg, 0.204 mmol) in CH_2Cl_2 (3 mL) was added dropwise to a suspension of hemiasterlin analog **A** as trifluoroacetatesalt[13] (30 mg, 0.051 mmol) and PyBOP (26.5 mg, 0.051 mmol) in CH_2Cl_2 (3 mL). The reaction mixture was stirred 24 h at room temperature before removing the solvent under reduced pressure. The product was first purified by column chromatography with (CH_2Cl_2/Toluene/MeOH, 17/2.2/0.5, R_{f1} 0.25) and then by preparative HPLC to give compound **A-L** as a colourless solid (27.5 mg, 89%).

R_{f2} (CH_2Cl_2/MeOH): 0.78

^{1}H NMR ($CDCl_3$): 0.76 (d, 3H, *J* = 7.2), 0.85 (d, 3H, J = 7.1), 0.99 (s, 9H), 1.12 (br, 3H), 1.40-1.51 (br, 8H), 1.82-1.90 (m, 1H), 1.92 (d, 3H, *J* = 1.2), 2.48-2.52 (m, 1H), 2.97 (s, 3H), 3.58-3.76 (m, 10H), 4.29-4.32 (m, 2H), 4.74 (d, 1H, *J* = 10), 5.09 (dd, 1H, *J* = 8 and 9.8), 6.67 (dd, 1H, *J*= 8 and 1.2), 7.19-7.43 (m, 5H), 8.12 (br s, 1H).

^{13}C NMR ($CDCl_3$): 13.9, 18.7, 19.5, 21.3, 21.4, 26.6, 26.7, 26.9, 30.0, 31.2, 35.3, 53.0, 54.7, 55.0, 61.8, 63.9, 69.2, 70.5, 70.7, 72.5, 110.2, 125.7, 126.8, 128.3, 132.4, 139.3, 167.7, 171.7, 173.1.

m/z: 606.709.

*Compound **A-L-B***. To a suspension of hemiasterlin analog **A** as trifluoroacetate salt[13] (0.04 g, 0.07 mM) in CH_2Cl_2 (2 mL) a solution of DIEA (0.05 mL, 0.27 mM), PyBOP (0.035 g, 0.07mM) and compound **B-L**[15] (0.035 g, 0.08 mM) in CH_2Cl_2 (3 mL) was added. The mixture was stirred over night at room temperature and then concentrated in vacuo to give a slurry that was first purified by column chromatography (PE/AcOEt, 1/3, R_f: 0.4) and then by preparative HPLC to give the product as a colourless solid (0.044 g, 69%).

^{1}H NMR ($CDCl_3$): 0.77 (d, 3H, *J* = 6.8), 0.86 (d, 3H, *J* = 6.8), 0.98 (s, 9H), 1.16 (br, 3H), 1.50 (br s, 7H), 1.83-1.91 (m, 1H), 1.92 (d, 3H, *J* = 0.8), 2.97 (s, 3H), 3.03 (m, 1H), 3.65 (s, 6H), 3.68-3.79 (m, 8H), 3.81 (s, 3H), 4.28-4.31 (m, 4H), 4.74 (d, 1H, *J* = 9.4), 5.10 (dd, 1H, *J* = 7.3 and 7.1), 6.29-6.30 (m, 1H), 6.37 (t, 1H), 6.43-6.46 (m, 5H), 6.66 (d, 1H, *J* = 8.4), 6.92 (dd, 1H; *J* = 7.3 and 0.8), 7.22-7.27 (m, 1H), 7.31-7.36 (m, 2H), 7.43-7.45 (m, 2H), 8.01 (br, 2H)

^{13}C NMR ($CDCl_3$): 14.0, 18.6, 18.9, 19.4, 25.0, 26.4, 27.4, 29.7, 29.8, 31.4, 35.8, 53.3, 55.3, 55.8, 56.2, 56.9, 63.6, 64.1, 64.3, 69.2, 69.6, 70.7, 99.7, 100.1, 106.8, 109.7, 119.3, 123.5, 126.3, 127.1, 129.2, 129.5, 129.9, 130.2, 130.5, 133, 137.8, 137.9, 160.6, 161.1, 167.4, 169.3, 171.0, 183.7

m/z: 917.398.

Materials. Taltobulin was purchased from MedKoo Biosciences (North Carolina, USA). Trifluoroacetic acid (TFA) and Celiprolol hydrochloride were obtained from Sigma-Aldrich Italia (Milan, Italy). Methanol, acetonitrile, ethyl acetate and water were high performance liquid chromatography (HPLC) grade from Sigma-Aldrich. McCoy's 5A medium and L-glutamine were purchased from Invitrogen Life Technologies (Carlsbad, CA, USA). Fetal bovine serum (FBS), Dulbecco's modified Eagle's medium (DMEM) + Glutamax, streptomycin and penicillin and phosphate-buffered saline (PBS) were obtained from Invitrogen (Life Technologies Italia, Milan, Italy). NCM-460 cells were kindly provided by Dr. Antonio Strillacci, University of Bologna, Italy.

Biological activities. An ovarian cancer cell line SKOV3 was used to compare the growth inhibitory effect of the hybrid compound ***A-L-B*** with ***A***, ***A-L***, and ***B***. SKOV3 cells were maintained in McCoy's 5A medium supplemented with 10% fetal bovine serum and 1.5 mM L-glutamine and seeded to a 96-well plate at 2500-3500 cells/well one day before drug treatment. Cells were then treated with various concentrations of compounds for 48 h and cell viability was measured by the MTT assay. Half maximal inhibitory concentration (IC_{50}) was calculated using Scientist software. Experiments were performed in triplicate and data were presented as mean ± S.E. of 2 to 5 independent experiments.

HPLC Analysis. The quantification of ***taltobulin***, ***celiprolol***, the hybrid compound ***A-L-B*** and its potential hydrolysis products ***A*, *A-L*, *B*, *B-L*** was performed by HPLC. The chromatographic apparatus consisted of a modular system (model LC-10 AD VD pump and model SPD-10A VP variable wavelength UV−Vis detector; Shimadzu,Kyoto, Japan) and an injection valve with 20 μL sample loop (model 7725; Rheodyne, IDEX, Torrance, CA, USA). Separations were performed at room temperature on a 5 μm Hypersil BDS C-18 column (150 mm × 4.6 mm *i.d*; Alltech Italia Srl, Milan, Italy), equipped with a guard column packed with the same Hypersil material. Data acquisition and processing were accomplished with a personal computer using CLASS-VP Software, version 7.2.1 (Shimadzu Italia, Milan, Italy). The detector was set at 220 nm for the analysis of the compounds ***A***, ***A-L*** and the hybrid ***A-L-B*,** whereas for the analysis of **celiprolol** it was set at 232 nm and, finally, at 270 nm for the analysis of the compounds ***B*** and ***B-L***. The mobile phase consisted of an isocratic mixture of water and acetonitrile in the presence of TFA 0.1% (v/v) with a ratio of 60:40 (v/v) for the analysis of the compounds ***A***, ***A-L***, ***B***, ***B-L*** and ***taltobulin***; the ratios were instead 70:30 and 10:90 (v/v) for the analysis of ***celiprolol*** and the hybrid ***A-L-B***, respectively. The kinetic analysis of the hybrid ***A-L-B*** degradation and its hydrolysis products release in rat whole blood or in liver homogenates were performed via HPLC with a mobile phase consisting of a mixture of water and acetonitrile in the presence of TFA 0.1% (v/v) regulated by a gradient profile programmed as follows: isocratic elution with a ratio 60:40 (v/v) for 14 min; then a 1-min linear gradient to the ratio 10:90 % (v/v); the mobile phase composition was finally maintained at the ratio 10:90% (v/v) for 6 min. After each cycle the column was conditioned with the ratio 60:40 (v/v) for 10 min. The flow rate was 1 mL/min. The compound *cis-3,4',5-trimethoxy-3'-hydroxystilbene* (***C***, Figure 1), was employed as internal standard for the analysis of rat blood and liver homogenates extracts.

The retention times obtained with the isocratic elutions were 4.82 min for the compounds ***A*** and ***B***, 5.30 min for the compound **A-L**; 9.80 min for the compound ***B-L*** and **12.10** min for the

internal standard C; 4.94 min for ***taltobulin***, 4.50 min for ***celiprolol***; 4.60 min for the hybrid ***A-L-B***. The retention times obtained with the elution regulated by the gradient profile were the same as previously reported for the compounds ***A***, ***A-L***, ***B***, ***B-L*** and the ***internal standard C***; the retention time of the hybrid ***A-L-B*** was instead 19.80 min. The quantification of the compound ***A*** released by the hydrolysis of the hybrid ***A-L-B*** was obtained by the difference of the peak area obtained at 220 nm at 4.82 min and the double of peak area obtained at 270 nm at the same retention time of the same injected sample. It has been indeed verified that the compound ***A*** was totally undetectable at 270 nm, whereas the mean ± S.D. of ratio of the peak areas of the compound ***B*** detected at 220 and 270 nm was 2.0 ± 0.1 in the concentration range between 5 μM and 50 μM (n = 6). This strategy was necessary being the retention times of the compounds ***A*** and ***B*** the same.

The chromatographic precision was evaluated by repeated analysis (n = 6) of the same sample solution containing each of the examined compound at a concentration of 10 μM. The solutes were dissolved in water, with the exception of the hybrid ***A-L-B*** dissolved in a mixture of water and methanol 50:50 (v/v). Calibration curves of peak areas versus concentration (n = 9) were generated in the range 1 to 300 μM for the compounds ***A*** and ***taltobulin***; in the range 0.5 to 100 μM for the compounds ***A-L***, ***B***, ***B-L***; in the range 1 to 100 μM for the hybrid ***A-L-B*** and in the range 0.25 to 200 μM for ***celiprolol***. The limit of quantification (LOQ) and detection (LOD) values were determined with a signal-to-noise ratio of 10 and 3 respectively.

Solubility determination. For determining solubility values, an excess amount of compound ***A*** (8 mg/mL) or hybrid ***A-L-B*** (3 mg/mL) was added to 3 mL of water and left to equilibrate at room temperature under continuous stirring for 36 h. After filtration the *sample* ***A-L-B*** was analyzed by HPLC, whereas the sample **A** was analyzed after dilution 1:100.

Kinetic analysis in culture medium. The compounds ***A***, ***A-L***, ***B***, ***B-L*** or the hybrid ***A-L-B*** were incubated at 37 °C in a mixture of DMEM supplemented with 10% FBS, 50 mg/mL streptomycin, and 50 IU/mL penicillin. The incubation phase (3 mL) was spiked with 10^{-2} M stock

solutions of the compounds in DMSO in order to obtain their final concentration of 50 μM. During the experiments, the samples were shaken continuously and gently in an oscillating water bath. At regular time intervals, 100 μL aliquots of samples were withdrawn and immediately quenched in 300 μL of ethanol (4°C); 100 μL of 50 μM ***internal standard C*** was then added. After centrifugation at 13000g for 10 min, 400 μL aliquots were reduced to dryness under a nitrogen stream and re-dissolved in 150 μL of water-methanol (50:50 v/v); after centrifugation, 10 μL was injected into the HPLC system for the quantification of the samples. All the values were obtained as the mean of three independent incubation experiments.

A preliminary analysis performed on blank samples showed that its components did not interfere with the retention times of the compounds analyzed. Recovery experiments were performed by comparing the peak areas of each 25 μM compound extracted from the DMEM mixture at 4 °C (n = 3) with those obtained by injection of an equivalent concentration of the analytes dissolved in the mixture water-methanol (50:50 v/v). The quantification of ***A***, ***A-L***, ***B***, ***B-L*** and the hybrid ***A-L-B*** was performed by a calibration curve constructed for each compound by employing six different standard solutions in DMEM mixture at 4 °C, ranging from 5 to 50 μM and plotted as analyte to internal standard peak area ratios versus concentration. The accuracy of the method was evaluated for each 25 μM compound with respect to their calibration curves (n = 6).

Kinetic Analysis in Rat Whole Blood. The compounds ***A***, ***A-L***, ***B***, ***B-L*** or the hybrid ***A-L-B*** were incubated at 37 °C in heparinized whole blood obtained from different rats (male Wistar, Harlan SRC, Milan, Italy) weighing 200−250 g. Three milliliters of whole blood was spiked with compound solutions resulting in final concentration of 50 μM, obtained by adding 5 μL of 10^{-2} M stock solution in DMSO for each milliliter incubated. During the experiments, the samples were shaken continuously and gently in an oscillating water bath. At regular time intervals, 100 μL of samples were withdrawn and immediately quenched in 500 μL of ice cold water; then 50 μL of 10% sulfosalicylic acid and 100 μL of 100 μM ***internal standard C*** were added. The samples were extracted twice with 1 mL of water saturated ethyl acetate, and, after centrifugation, the organic

layer was reduced to dryness under a nitrogen stream. Two hundred microliters of a water and methanol mixture (50:50 v/v) was added, and, after centrifugation, 10 μL was injected into the HPLC system. All the values were obtained as the mean of three independent incubation experiments. A preliminary analysis performed on blank samples showed that its components did not interfere with the retention times of the compounds analyzed.

Recovery experiments were performed by comparing the peak areas of each 25 μM compound extracted from the rat whole blood at 4 °C (n = 3) with those obtained by injection of an equivalent concentration of the analytes dissolved in the mixture water−methanol (50:50 v/v). The quantification of ***A***, ***A-L***, ***B***, ***B-L*** and the hybrid ***A-L-B*** was performed by a calibration curve constructed for each compound by employing six different standard solutions in rat whole blood at 4 °C, ranging from 5 to 50 μM and plotted as analyte to internal standard peak area ratios versus concentration. The accuracy of the method was evaluated for each 25 μM compound with respect to their calibration curves (n = 6).

Preparation of Rat Liver Homogenates. The livers of male Wistar rats were immediately isolated after their decapitation, washed with ice cold saline solution, and homogenized in 4 volumes (w/v) of TrisHCl (50 mM, pH 7.4, 4 °C) with a Potter-Elvehjem apparatus (Vetrotecnica, Padova, Italy). The supernatant obtained after centrifugation (2000g for 10 min at 4 °C) was decanted off and stored at −80°C before its employment for kinetic studies. The total protein concentration in the tissue homogenate was determined using the Lowry procedure[16] and resulted as 31.8 ± 1.3 μg of protein/μL.

Kinetic Analysis in Rat Liver Homogenates. The compounds ***A***, ***A-L***, ***B***, ***B-L*** or the hybrid ***A-L-B*** were incubated at 37 °C in 3 mL of rat liver homogenates, resulting in a final concentration of 50 μM, obtained by adding 15 μL of 10^{-2} M stock solution in DMSO. During the experiments, the samples were shaken continuously and gently in an oscillating water bath. At regular time intervals, 100 μL aliquots of samples were withdrawn and immediately quenched in 300 μL of ethanol (4°C); 100 μL of 100 μM ***internal standard C*** was then added. After centrifugation at

13000g for 10 min, 400 μL aliquots were reduced to dryness under a nitrogen stream and redissolved in 150 μL of water-methanol (50:50 v/v), and, after centrifugation, 10 μL was injected into the HPLC system. All the values were obtained as the mean of three independent incubation experiments. A preliminary analysis performed on blank samples showed that its components did not interfere with the retention times of the compounds analyzed.

Recovery experiments were performed by comparing the peak areas of each 25 μM compound extracted from the rat liver homogenates at 4 °C (n = 3) with those obtained by injection of an equivalent concentration of the analytes dissolved in the mixture water-methanol (50:50 v/v). The quantification of ***A***, ***A-L***, ***B***, ***B-L*** and the hybrid ***A-L-B*** was performed by a calibration curve constructed for each compound by employing six different standard solutions in rat liver homogenates at 4 °C, ranging from 5 to 50 μM and plotted as analyte to internal standard peak area ratios versus concentration. The accuracy of the method was evaluated for each 25 μM compound with respect to their calibration curves (n = 6).

Kinetic Calculations. The half-life values of the compounds showing a first order kinetic degradation were calculated from an exponential decay plot of its concentrations versus incubation time, using the computer program GraphPad Prism (GraphPad, San Diego, CA). The same software was employed for the linear regression of the corresponding semilogarithmic plots. The quality of the fits was determined by evaluating the correlation coefficients (r) and P values.

Cell Culture. The NCM460 cell line was grown in DMEM + Glutamax supplemented with 10 % fetal bovine serum (FBS), 100 U/mL penicillin and 100 μg/mL streptomycin at 37 °C in a humidified atmosphere with 5% of CO_2. For maximum viability, NCM460 cells were subcultured in fresh and spent growth medium in 1:1 ratio.

RNA extraction and Reverse transcription PCR. Total RNA was isolated from 10 million of cells. The cells were lysed in 1 ml of TRIzol Reagent (Invitrogen, Carlsbad, CA, USA) by pipetting. After incubation of the homogenized samples for 5 min at room temperature, 0.2 ml of chloroform

was added. The samples were mixed vigorously and then centrifuged at 12,000 × g for 15 min at 4°C. The RNA was precipitated from the aqueous phase at room temperature by adding 0.5 ml of isopropanol and centrifuging at 12,000 × g for 10 min at 4°C. The RNA pellet was washed once with 75% ethanol and the pellet was air dried and dissolved in diethyl pyrocarbonate (DEPC)-treated water. The RNA concentration was determined by measure the optical absorbance at 260 nm. Reverse transcription was performed from 2 μg of total RNA using ImProm-II™ (Promega, Madison, WI, USA) using a mixture of oligo-dT and random-primers in a final volume of 20 μl. To perform the PCR reactions 0.5 μl aliquots of cDNA and the following forward and reverse gene specific primers were used: ABCB1, Homo sapiens ATP-binding cassette, sub-family B, member 1 (5'-ATG TTT CCG GTT TGG AGC CT-3' / 5'-TCC TTC CAA TGT GTT CGG CA-3'); ABCC1, Homo sapiens ATP-binding cassette, sub-family C, member 1 (5'-CCT GAA GGT GGA CGA GAA CC-3' / 5'-TGT GCC TGA GAA CGA AGT CC-3'); ABCG2, Homo sapiens ATP-binding cassette, sub-family G, member 2 (variant 1, 5'-CTC CCA TCG TGA CCT CCA GC-3' / 5'-TCA TTG GAA GCT GTC GCG GG-3'; variant 2, 5'-GGG TAA TCC CCA GGC CTC TA-3' / 5'-TGA GAT TGA CCA ACA GAC CAT CA-3'). The forward and reverse primers were designed in exons separated by a long intronic sequence in order to rule out amplification from genomic DNA. Briefly, 25 μl of PCR mixture, containing 0.4 μM primers, 2.5 mM $MgCl_2$, 0.4 mM deoxynucleoside triphosphates, 0.2 μl DyNAzyme II DNA Polymerase (Finnzymes, Espoo, Finland), were amplified by using a T100 thermal cycler (Bio-Rad Laboratories, Hercules, CA). The thermal cycler conditions included initial denaturation of 30 s and then 28 cycles of 95°C for 10 s, 62°C for 30 s for annealing, and 72°C for 45 s. PCR products were separated on 2 % agarose gel, stained with ethidium bromide and examined with UV light and visualized with a Gel Doc 1000 Documentation System (Bio-Rad Laboratories, Hercules, CA). Amplification of human Actin, GAPDH and HMBS housekeeping genes was performed in parallel PCR reactions in order to confirm the quality of cDNA. Negative controls (no template cDNA) were also run with every experimental plate to assess specificity and to rule out contamination.

Differentiation of NCM460 Cells to Polarized Monolayers. Differentiation to NCM460 cell monolayers was performed modifying the method reported by Dalpiaz and co-workers.[17] Briefly, after two passages, confluent NCM460 cells were seeded at a density of 10^5 cells/mL in 1:1 ratio fresh and spent culture medium in 12-well Millicell inserts (Millipore, Milan, Italy) consisting of 1.0 μm pore size polyethylene terephthalate (PET) filter membranes, whose surface was 1.12 cm^2. Filters were presoaked for 24 h with fresh culture medium, and then the upper compartment (apical, A) received 400 μL of the diluted cells, whereas the lower (basolateral, B) received 2 mL of the medium in the absence of cells. Half volume of the culture medium was replaced every two days with fresh medium to each of the apical and basolateral compartments. The integrity of the cell monolayers was monitored by measuring the transepithelial electrical resistance (TEER) by means of a voltmeter (Millicell-ERS; Millipore, Milan, Italy). The measured resistance value was multiplied by the area of the filter to obtain an absolute value of TEER, expressed as $\Omega \cdot cm^2$. The background resistance of blank inserts not plated with cells was around 35 $Ù \cdot cm^2$ and was deducted from each value. The homogeneity and integrity of the cell monolayer were also monitored by phase contrast microscopy. Based on these parameters, cell monolayers reached confluence and epithelial polarization after 6 days and monolayers with TEER stable value of 180 ± 11 $Ù \cdot cm^2$ were used for permeation studies. At this time, the medium was replaced with low serum fresh medium (1 % FBS) in both the apical and basal compartments where it was leaved for 24 hours before permeation experiments.

Permeation Studies Across Cell Monolayers. Permeation experiments were performed in triplicate in both the apical-to basolateral (A → B) and basolateral to apical (B → A) directions. For these studies, solutions of compounds ***A***, ***celiprolol*** and ***taltobulin*** were prepared in PBS containing 5 mM glucose at a concentration of 100 μM, obtained by adding 5 μL of $2 \cdot 10^{-2}$ M stock solution in DMSO for each milliliter incubated. The culture low serum fresh media of NMC460 cell monolayers were removed from both the A and B sides of the inserts and both sides were washed

twice with prewarmed PBS. During transport experiments the Millicell systems were continuously swirled on an orbital shaker (100 rpm) at 37 °C. For the A → B permeation studies 0.4 mL of compound ***A***, ***celiprolol***, or ***taltobulin*** solutions were added to apical side at time t = 0 and the inserts were placed in the cell culture plate whose basolateral compartment was prefilled with 2 mL of prewarmed PBS containing 5 mM glucose. At programmed time points the inserts were removed and transferred to a new well plate containing fresh PBS with glucose. The basolateral contents were collected after the insert removal and 10 µL aliquots of filtered (0.45 µm) samples were immediately injected into the HPLC apparatus. For the B → A permeation studies 2 mL of compound ***A***, ***celiprolol***, or ***taltobulin*** solutions were placed on the basolateral side of Millicell inserts at time t = 0, whereas the apical side contained 0.4 mL of fresh PBS with glucose. At predetermined time points, the apical samples were removed and replaced with fresh PBS containing glucose. The collected apical samples were immediately filtered (0.45 µm) and injected (10 µl) into the HPLC apparatus. The TEER values were monitored before and after each experiment. Permeation studies were also conducted using cell-free inserts in the same conditions described above. All the values obtained were the mean of three independent experiments.

Apparent permeability coefficients (P_{app}) of the analyzed compounds were calculated according to the following equation:[18-20]

$$P_{app} = \frac{\frac{dc}{dt} V_r}{S_A C_o} \qquad [1]$$

where P_{app} is the apparent permeability coefficient in cm/min; dc/dt is the flux of drug across the filters, calculated as the linearly regressed slope through linear data; V_r is the volume in the receiving compartment (Apical = 0.4 mL; Basolateral = 2 mL); S_A is the diffusion area (1.13 cm^2); and C_0 is the initial compound concentration in the donor chamber at t = 0.

The permeabilities were determined for the filters alone (P_f) and for the filters covered by cells (P_t). The apparent permeability coefficients P_E referred to the cellular monolayer were then

calculated as follows:[19,21]

$$\frac{1}{P_E} = \frac{1}{P_t} - \frac{1}{P_f} \quad [2]$$

Statistical Analysis. Statistical comparisons of permeability coefficients or cumulative concentrations obtained from the transport studies were made by one way ANOVA or Student's t test (GraphPad Prism). $P < 0.05$ was considered statistically significant. GraphPad Prism was employed for the linear regression of the cumulative amounts of the compounds in the receiving compartments of the Millicell systems. The quality of fit was determined by evaluating the correlation coefficients (r) and P values.

RESULTS

Chemistry. The syntheses of single diastereoisomers of compounds ***A-L*** and ***A-L-B*** were performed, respectively, as depicted in Schemes 1 and 2. The synthesis of hemiasterlin congener ***A*** represented the most challenging synthetic sequence in both Schemes. In this route the key-step consists in an Ag_2O-promoted nucleophilic subtitution[22] on chiral non-racemic precursor 2-bromo-derivative *(R)(S)(S)*-**3**, in turn obtained by condensation of 2-bromoacid *(R)*-**1** with dipeptide *(S)(S)*-**2**. Bromine displacement by 2-phenyl-2-propanamine afforded, with the desired regio- and stereochemistry, tripeptide-ester *(R)(S)(S)*-**4** that was hydrolized with LiOH to obtain hemiasterlin derivative ***A***. The carboxy group of ***A*** was reacted by standard procedures with triethylene glycol to give the corresponding ester ***A-L*** in good yield.

In Scheme 2, the amino-stilbene ***B*** has been quite easly prepared as previously described, through a Wittig reaction between opportune phosphonium salt and aldehyde. *Cis*-stereoisomer formed in minor yield with respect to *Trans*-stereoisomer (1:2 ratio) but, being the only active isomer, it was isolated by flash chromatography. By reaction with trichloromethyl chloroformate,

the amino group of ***B*** was derivatized to isocianate (*Cis*-**5**) and, without purification, condensed with triethylene glycol to obtain the carbamate *Cis*-**6**.[15] Esterification of ***A*** at the *C*-terminus with hydroxy group of *Cis*-**6** produced the hybrid compound ***A-L-B***.

Biological activities. Previous studies indicated that the IC_{50} values of compound ***A*** ranged from 10 to 20 nM,[13,14] and compound ***B*** from 15 to 30 nM in UCI-101 human ovarian cancer cells,[14,15] whereas compound ***B-L*** was inactive and had an IC_{50} value greater than 10,000 nM in the same cell line. Here we compared the potencies of compounds ***A***, ***B***, ***A-L*** and ***A-L-B*** in another human ovarian cancer cell line, SKOV3, treated with various concentrations of compounds for 48 h, followed by the MTT assay. The obtained IC_{50} values were 7.48 ± 1.27 nM for compound ***A*** (n = 5), 40.3 ± 6.28 nM for compound ***B*** (n = 2), 738 ± 38.5 nM for compound ***A-L*** (n = 3), and 37.9 ± 2.11 nM for compound ***A-L-B*** (n = 2). Similar to ***B-L***, ***A-L*** was much less potent compared to compound ***A***. All together, these results suggest that the presence of a ***linker*** may block the activity of both compounds ***A*** and ***B*** and the ***linker*** is not hydrolyzed in the *in vitro* cell culture system. However, the hybrid compound ***A-L-B*** was much more potent than ***A-L*** or ***B-L***, and has IC_{50} very close to that of compound ***B*** under cell culture conditions.

HPLC analysis. A first step of our work was the evaluation of the potential hydrolysis pattern of the hybrid compound ***A-L-B*** in different media such as culture medium for cells, rat whole blood or rat liver homogenates. In this aim it was necessary to detect and quantify in all incubation media not only the hybrid compound ***A-L-B***, but also its potential hydrolysis products ***A***, ***A-L***, ***B*** and ***B-L***. In order to do so, an efficacious analytical method was developed via HPLC-UV based on the employment of a reverse phase C-18 HPLC column and a mobile phase constituted by a mixture of water and acetonitrile in the presence of TFA 0.1% (v/v) following a gradient profile. In particular, the mixture water-acetonitrile 60:40 (v/v), programmed for the first 14 min, allowed the detection of the compounds ***A***, ***A-L***, ***B***, ***B-L*** and the ***internal standard C***, whereas the mixture water-acetonitrile (10:90), programmed for the following 6 min, allowed the detection of the hybrid ***A-L-B***. No interferences were observed from culture medium, whole blood and liver homogenate

extract components. Therefore, this gradient profile allowed us to quantify both the hybrid ***A-L-B*** and its hydrolysis products ***A***, ***A-L***, ***B*** and ***B-L*** in the same HPLC chromatograms in all incubation media investigated. Moreover, the isocratic elution with the mixture water−acetonitrile 60:40 (v/v) allowed to quantify the compounds ***A-L*** and ***B-L*** together with their potential hydrolysis products, ***A*** and ***B***, respectively, in a same HPLC chromatogram in all incubation media investigated.

In the second step of our work we have performed diffusion studies of the compound ***A*** across NMC460 cell monolayers in order to evaluate its potential ability to interact with active efflux transporters (AET), whose activity can induce multidrug resistance (MDR).[23] We have validated by HPLC the NMC460 cell monolayers for transport studies with the use of reference compounds, such as ***celiprolol***, known as a P-gp substrate,[24] and ***taltobulin***, known for its ability to elude this type of AETs.[10] We have therefore developed an HPLC analytical method also for these compounds, whose quantification was obtained by isocratic elution using appropriate mixtures of water-acetonitrile in the presence of TFA 0.1% (v/v).

The chromatographic precision for all analyzed compounds were represented by their relative standard deviation (RSD), whose values ranged between 0.89% and 0.96%. The calibration curves of the same compounds were linear ($n = 9$, $r > 0.996$, $P < 0{,}0001$) in the concentration ranges investigated.

The limits of quantification (LOQ) with a signal-to-noise ratio of 10 were 1.0 μM (5.9 ng injected) for ***A***; 0.5 μM (3.0 ng injected) for ***A-L***; 0.15 μM (0.5 ng injected) for ***B***; 0.089 μM (0.4 ng injected) for ***B-L***; 0.9 μM (9,3 ng injected) for the hybrid ***A-L-B***; 0.25 μM (0.95 ng injected) for ***celiprolol***; 0,6 uM (2.8 ng injected) for ***taltobulin***. The limits of detection (LOD) with a signal-to-noise of 3 were 0.3 μM (1.8 ng injected) for ***A***; 0.15 μM (0.9 ng injected) ***A-L***; 0.05 μM (0.15 ng injected) for ***B***; 0.027 μM (0.12 ng injected) for ***B-L***; 0.27 μM (2.8 ng injected) for the hybrid ***A-L-B***; 0.08 μM (0.29 ng injected) for ***celiprolol*****;** 0.18 uM (0.84 ng injected) for ***taltobulin***.

The solubility values of compound **A** and the hybrid **A-L-B** in water were 7.7 ± 0.5 mM (4.5 ± 0.03 mg/ml) and 14.5 ± 0.7 μM (0.015 ± 0.001 mg/ml), respectively.

The average recoveries ± SD of 10 μM compounds from rat whole blood were 91 ± 4% for ***A***; 53 ± 3% for ***A-L***; 24 ±1% for ***B***; 95 ±4% for ***B-L*** and 39 ±4% for the hybrid ***A-L-B***. The average recoveries ± SD of 10 μM compounds from the medium for cell culture or from rat liver homogenates were ≥ 92 ± 4% for ***A***; ≥ 84 ± 3% for ***A-L***; ≥ 41% ± 3 for ***B***; ≥ 91 ± 5% for ***B-L*** and ≥ 54 ± 3% for the hybrid ***A-L-B***. The concentrations of these compounds were therefore referred to as peak area ratio with respect to their internal standard. The precision of the method based on peak area ratio was represented by RSD values ranging between 1.05% and 1.64% for 10 μM compounds extracted from the different incubation media; their calibration curves were linear over the range 5−50 μM ($n = 6$, $r > 0.992$, $P < 0.0001$). The assay accuracy values were described for these compounds by relative errors comprised between −2.64% and 1.68%.

Hydrolysis and stability studies. The compounds ***A***, ***A-L***, ***B***, ***B-L*** and ***A-L-B*** were not degraded in the mixture of DMEM supplemented with FBS, streptomycin and penicillin, a medium employed for growth inhibition studies of several cancer cell lines.[15]

The compounds ***A*** and ***B*** incubated at 37°C in rat whole blood, or rat liver homogenates were not degraded within eight hours (Figures 2 and 4). However, at the same experimental conditions, the compounds ***A-L***, ***B-L*** and the hybrid ***A-L-B*** appeared degraded, showing different half lives in dependence of the types of compound and incubation medium. Figure 2 reports the degradation profiles in rat whole blood of the compounds ***A-L***, ***B-L*** and the hybrid ***A-L-B***, whose half lives were 25.4 ± 1.1 min, 288 ± 12 min and 118.2 ± 9.5 min, respectively. The degradations followed pseudo first-order kinetics, confirmed by the linear patterns of corresponding semi-logarithmic plots ($n = 9$, $r \geq 0.990$ $p < 0.0001$) and suggesting, therefore, their degradation governed by hydrolysis processes. The hydrolysis of these compounds was confirmed by the appearance in incubation media of their degradation products. In particular, as reported in Figure 3A and 3B, the degradation of ***A-L*** and ***B-L*** were accompanied by the appearance and timed increase of their

hydrolysis products ***A*** and ***B***, respectively: after 100 min of incubation in rat whole blood, the compound ***A-L*** appeared totally hydrolyzed, whereas the incubation of ***B-L*** for 450 min allowed to degrade about the 70% of its starting amount, showing the appearance of a corresponding amount of its hydrolysis product ***B***. As reported in Figure 3C, the degradation of the hybrid ***A-L-B*** was accompanied by the appearance of the compounds ***A*** and ***B-L*** with increasing patterns during time, but not by the appearance of the compound ***A-L***. This result indicates that the urethanic bond between ***B*** and the ***linker*** was not hydrolyzed by rat whole blood, differently from the ester bond between ***A*** and the ***linker***. As evidenced in Figure 3C, the amounts of ***A*** released during time in rat whole blood, appeared to correspond with those of the hybrid ***A-L-B*** degraded. The ***B*** appearance during incubation of ***A-L-B*** in rat whole blood (Figure 3C) was therefore due to the hydrolysis ***B-L***, released during the degradation of the hybrid compound.

In rat liver homogenates the compounds ***A-L***, ***B-L*** and the hybrid ***A-L-B*** were hydrolyzed with patterns similar to those observed in rat whole blood, even if characterized by significantly lower rates of degradation. Indeed, as reported in Figure 4, during eight hours of incubation, less than 30% of the compounds ***B-L*** and ***A-L-B*** were degraded, whereas more than the 95% of the compound ***A-L*** was degraded, showing an half life of 118.0 ± 7.2 min. In Figure 5 it is evidenced that the degradation of these compounds is due to hydrolysis processes and, as observed in rat whole blood, only the ester bond between ***A*** and the ***linker*** of the hybrid ***A-L-B*** was hydrolyzed.

Millicell permeation studies. The results above indicate that the hybrid ***A-L-B*** is hydrolyzed in physiologic fluids, allowing a relatively fast release of the compound ***A*** which is characterized by a potent anti-microtubule activity. This drug is a derivative of ***taltobulin***, a known anti-cancer agent able to elude the AET systems,[10,12] whose overexpression by cancer cells induces the MDR phenomenon.[23, 25] It has been therefore crucial to verify whether compound ***A*** was able to elude the AET systems and the related MDR phenomenon. To this aim we have employed the human NCM460 cell line to study the potential interaction of ***A*** with the active efflux transporters. Control experiments were first performed to provide evidences that NCM460 cells monolayer is an

useful model for drug transport studies. Firstly, we analyzed in NCM460 cells the expression of active efflux transporters P-gP, MRP1 and BCRP by RT-PCR (Figure 6). The analysis has been performed on the total RNA by using specific primers recognizing the genes ABCB1 (P-gP), ABCC1 (MRP1), and ABCG2 - variant 1 and variant 2 – (BCRP). Since amplified products of the expected size were obtained only for ABCB1 (250 bp) and ABCC1(490 bp) genes, we deduced that NCM460 cells expressed the P-gp and MRP1 active efflux transporters. In addition, the expression and activity of P-gp transporters on NCM460 cells was validated by permeation experiments achieved with the P-gP substrate ***celiprolol***.[24] In particular, transport studies were performed in both the apical-to basolateral (A → B) and basolateral to apical (B → A) directions after cell cultures reached the confluence, using parallel sets of Millicell well plates with similar TEER values (180 ± 11 $\Omega \cdot cm^2$). The permeation profiles of ***celiprolol*** across the Millicell filters alone or coated by monolayers obtained by NCM460 cells are reported in Figure 7a, where the cumulative concentrations in the receiving compartments are shown. The profiles describe the transport from the apical to basolateral compartments (A → B) and vice versa. The cumulative amounts of ***celiprolol*** in the receiving compartments showed a linear profile within 120 min in all cases ($r \geq 0.998$, $P \leq 0.001$) indicating constant permeation conditions during this range of time. The resulting slopes of the linear fits were used in eq 1 for calculation of permeability coefficients (P_t and P_f) that were employed to calculate, according to eq 2, the apparent permeability coefficients (P_E) of ***celiprolol*** specific for the cellular monolayers, reported in Table 1. The P_E values for A → B and B → A transport of ***celiprolol*** were $2.95 \pm 0.06 \times 10^{-4}$ and $9.98 \pm 0.56 \times 10^{-4}$ cm/min, respectively. The permeation rate of this drug from the basolateral to the apical compartments appeared therefore about four times higher than its permeation rate from the apical to basolateral compartments ($P < 0.001$), indicating the expression of the active efflux transporter P-gp in NCM460 cellular monolayers. Finally, transport studies on NCM460 cells monolayer have been also performed with ***taltobulin***, a reference drug able to elude the P-gp transporter.[10] The permeation profiles of this drug from the apical to basolateral compartments (A → B) and vice

versa, are reported in Figure 7b. The cumulative amounts of ***taltobulin*** in the receiving compartments showed a linear profile within 120 min in all cases ($r \geq 0.998$, $P \leq 0.002$) indicating constant permeation conditions during this range of time. In this case, the P_E values for A → B and B → A transport were $6.21 \pm 0.28 \times 10^{-4}$ and $6.96 \pm 0.24 \times 10^{-4}$ cm/min, respectively (Table 1). The permeation rate of ***taltobulin*** from the basolateral to the apical compartments appeared therefore the same with respect to its permeation rate from the apical to basolateral compartments ($P > 0.05$), indicating the ability of this drug to elude the AET systems, as reported in literature.[11] Taken together, the data reported in Table I and Figures 6-7 suggests that NCM460 cells monolayer is an useful model for drug transport studies.

We then employed this model for transport studies of the compound ***A***. The permeation profiles of this drug from the apical to basolateral compartments (A → B) and vice versa, are reported in Figure 7c. The cumulative amounts of compound ***A*** in the receiving compartments showed a linear profile within 120 min or 150 min in all cases ($r \geq 0.958$, $P < 0.001$) indicating constant permeation conditions during these ranges of time. In this case, the P_E values for A → B and B → A transport were $5.28 \pm 0.44 \times 10^{-4}$ and $7.96 \pm 0.37 \times 10^{-4}$ cm/min, respectively (Table 1). The permeation rate of this drug from the basolateral to the apical compartments appeared therefore about 1.5 times higher than its permeation rate from the apical to basolateral compartments ($P < 0.01$), showing a behavior more similar to that of ***taltobulin*** than that of ***celiprolol***. Analysis of the ratios between the P_E values referred to the basolateral → apical and apical → basolateral directions is reported in Table 1: the values were 3.4 ± 0.2 for ***celiprolol***, 1.12 ± 0.06 for ***taltobulin*** and 1.5 ± 0.1 for compound ***A***. The celiprolol value was statistically higher than those of ***taltobulin*** and ***compound A*** ($p < 0.001$) which did not appear dissimilar among them ($p > 0.05$). These data indicate that compound A did not interact with AET systems.

DISCUSSION

We have previously demonstrated that the hemiasterlin derivative ***A*** synergizes with the stilbene derivative ***B***, in their anti-microtubule activity.[14] The synergizing effect of the compound ***A*** with ***B*** is similar to that showed by hemiasterlins with *vincristine,* but a modeling approach suggested that compound ***A*** does not fit into the *vinca alkaloids* binding pocket of β-tubulin.[14] Recently, the binding site of hemiasterlins was identified on *α*-tubulin in a position very close to the *α/β* tubulin interface. Hemiasterlins therefore are capable of influencing both the vincristine binding site on *β*-tubulin,[26-28] and the c*olchicine* binding site at *α/β* interface, thus explaining their synergism with v*incristine* and ***B***.[14]

Taking into account these modes of interaction, this study proposes a conjugation of the compounds ***A*** and ***B*** in order to investigate the potential antitumor activity of the conjugate or its ability to be prodrug of the parent compounds. We have previously demonstrated that the conjugation strategy between active drugs can modulate their pharmacological activities and achieve their controlled release through hydrolysis processes occurring in the physiologic fluids.[29] We have also shown that drug conjugation with essential nutrients can allow to obtain prodrugs able to interact with carrier mediated transporters (CMT) for targeting to specific compartments of the body.[30-34] In addition, conjugation of an antiviral drug with a bile acid allows a prodrug to elude active efflux transporters (AET), whose expression in cell membranes is often related to MDR and inability of active agents to reach the central nervous system. [17] The prodrug obtained via bile acid conjugation was highly lipophilic, thus it appeared suitable to be encapsulated in micro or nanoparticulate systems useful for targeting strategies in the body.[23,35,36] Furthermore, the hybrid approach , in which at least one component targets tubulin, may produce improved clinical outcome of anticancer therapies.[37] In this prospective, we analyzed the characteristics of the hybrid compound obtained by ***A*** and ***B*** conjugation in order to evaluate its potential involvement for activity modulation, controlled release and targeting approaches of anticancer agents.

Due to the issue that the water solubility of the stilbene derivative ***B*** is very poor (< 1mg/ml),[15] a hydrophilic spacer ***L*** (triethylenglicole) was used for conjugation with the hemiasterlin derivative **A**. We have previously shown that the compound ***B-L*** (obtained by the ***B*** conjugation with the spacer ***L*** in order to increase its water solubility) did not inhibit cell growth, probably due to its inability to fit into the colchicine binding pocket.[15] In the present study, the IC_{50} value of the hemiasterlin derivative ***A*** (about the inhibition of SKOV3 cells growth) increased of two order of magnitude (from 7.48 ± 1.27 nM to 738 ± 38.5 nM) after conjugation with the spacer ***L*** (compound ***A-L***). The presence of the spacer seems to create difficulty in fitting with the hemiasterlin binding site. However, the hybrid ***A-L-B*** showed an IC_{50} value of 37.9 ± 2.11 nM, similar to that of compound ***B*** (40.3 ± 6.28 nM), suggesting that a synergism between ***A*** and ***B*** is still present in their conjugate form. These results suggest a further investigation of the length of the spacer, which may modulate the synergic effect of the ***A-B*** conjugates.

The poor activity of the compounds ***A-L*** and ***B-L*** suggests that the linker ***L*** is not hydrolyzed in the cell culture system to release free ***A*** or ***B***. In this study we have demonstrated that compounds ***A***, ***A-L***, ***B***, ***B-L*** and ***A-L-B*** are not degraded in a medium employed for growth inhibition studies of several cancer cell lines. In order to evaluate if these compounds can be potentially degraded after their administration in the body, we analyzed their pharmacokinetics in rat whole blood and liver homogenates *in vitro*. These studies showed that compounds ***A*** and ***B*** had high stability in physiologic fluids, whereas the compounds ***A-L***, ***B-L*** and ***A-L-B*** were hydrolyzed with different rates. In particular, the compound with the fastest hydrolysis was ***A-L***, which has an ester bond between the drug and the linker (half lives = 25.4 ± 1.1 min and 118.0 ± 7.2 min in whole blood and rat liver homogenates, respectively). On the other hand, the ***B-L*** hydrolysis was the slowest among the conjugates incubated in the physiologic fluids (half live = 288 ± 12 min in whole blood, about 20% of degradation within eight hours in liver homogenates), indicating the difficulties of endogenous enzymes to hydrolyze the urethane bond between the ***B*** and ***L***, in comparison with the ester bond between ***A*** and ***L***. This pattern was also confirmed by the hydrolysis

profile of the hybrid compound ***A-L-B***. Indeed, only its ester bound between ***A*** and ***L*** moieties was hydrolyzed with rates intermediate between those referred to ***A-L*** and ***B-L*** (half live = 118.2 ± 9.5 min in whole blood, about 30% of degradation within eight hours in liver homogenates), whereas any hydrolysis was observed for the urethane bond between ***B*** and ***L*** moieties. The slow ***B*** release in the incubation fluids of ***A-L-B*** was attributed to the hydrolysis of ***B-L***, which was released after the hydrolysis of the ester bound between the ***A*** and ***L*** moieties of ***A-L-B***. In accordance with our results, the biodegradation of poly(ester-urethane)s in blood appears mainly due to the breakage of their ester bonds, whereas urethane bonds can only be hydrolyzed depending on the joining agents chosen for their synthesis.[38]

The pharmacokinetic studies of ***A-L-B*** suggested its ability have a prolonged release of compound ***A*** in physiologic fluids. This compound is characterized by a potent anticancer activity, similar to that of *taltobulin,* currently considered the reference anticancer drug among the hemiasterlin derivatives.[12] Whereas the *taltobulin* enantioselective synthesis appears very difficult,[11,13] compound ***A*** is obtained by a versatile approach.[13] It is therefore important to investigate on the properties of this compound, taking into account that its prolonged release induced by ***A-L-B*** hydrolysis can open new perspectives for targeting strategies. Indeed, we have evidenced that the water solubility of ***A-L-B*** is very poor (0.015 ± 0.001 mg/ml with respect to 4.5 ± 0.03 mg/ml referred to compound ***A***), a property generally useful for drug loading in nanoparticulate polymeric systems.[39-42] Properly designed nanoparticles have the ability to accumulate in tumors by either passive or active targeting,[23] reducing concentration of anticancer drugs in healthy tissues with respect to conventional formulations and significantly enhancing selective cytotoxic effect of various antitumor agents.[43] ***A-L-B*** encapsulated in nanoparticles may therefore constitute a carrier able to induce a selective targeting and prolonged release of compound ***A*** in tumoral tissues. Thus, it is interesting to know if this compound, as *taltobulin*,[10] is potentially able to overcome MDR, a phenomenon that can be induced by an overexpression of active efflux transporters (AETs) on cancer cell membranes during chemotherapies. Anticancer agents that are

not substrates of AETs are in general able to elude MDR. We have therefore analyzed what is the behavior of compound ***A*** in this regard. In this aim, we have selected the human normal colonic epithelial NCM460 cells, which after confluence in millicell systems are able to acquire functional polarization, characterized by epithelial barrier properties.[44,45] In particular, the NCM460 cell layer separates an upper (apical) from a lower (basolateral) compartment. This system was efficaciously employed by us for *in vitro* permeation studies, in order to evaluate if drugs can be substrates of AETs. We have indeed demonstrated by RT-PCR analysis that NCM460 cells express the P-gp and MRP1 active efflux transporters, the main AETs involved in MDR phenomena.[23] This expression was then validated by permeation experiments achieved with the P-gP substrate ***celiprolol***,[24] whose apparent permeability coefficients (P_E) were found to be $2.95 \pm 0.06 \times 10^{-4}$ and $9.98 \pm 0.56 \times 10^{-4}$ cm/min for its permeation from apical (A) to basolateral (B) compartments and from B to A compartments, respectively. The latter data confirmed the presence of AET activity on NCM460 cells, as an higher permeation rate of ***celiprolol*** from the basolateral to apical sides of the millicell system, with respect to its permeation rate in the opposite direction. Any AET activity was instead observed for ***taltobulin*** during permeation studies across NCM460 monolayers, confirming the suitability of this system to evaluate the aptitude of drugs to be substrates of active efflux transporters. Thus, the permeation studies of compound ***A*** across NCM 460 monolayers indicated that this hemiasterlin derivative is not a substrate of P-gp active transporters, suggesting its potential ability of overcome MDR phenomena.

CONCLUSIONS

The hybrid compound ***A-L-B*** obtained by the conjugation of the hemiasterlin derivative ***A*** and the stilbene derivative ***B*** using triethylenglicole (***L***) as a spacer, showed anticancer activity with a potency similar to that of compound ***B*** and an order of magnitude lower than that of compound ***A***.

On the other hand, the presence of the spacer ***L*** in compounds ***A-L*** and ***B-L*** induced a drastic decrease of their anticancer activity. Compounds ***A*** and ***B*** are known to synergize their activity and this phenomenon appears to be maintained in the hybrid form. In rat whole blood the hybrid ***A-L-B*** is able to induce a sustained release of the compound ***A*** by hydrolysis of its ester bond with ***L***. The hydrolysis of the urethane bond between ***B*** and ***L*** has been observed only for the compound ***B-L*** and it induced a slow release in rat whole blood of the compound ***B***. We have demonstrated that the main hydrolysis product of ***A-L-B***, i.e. the hemiasterlin derivative ***A***, is not a substrate of active efflux proteins, suggesting its ability to elude the MDR phenomenon. The poor water solubility of ***A-L-B*** indicates this hybrid as a good candidate for encapsulation studies in nanoparticulate formulations, in order to obtain carriers able to induce its selective targeting in tumoral tissues, where a prolonged release of compound ***A*** should induce potentially efficacious and selective anticancer effects.

REFERENCES

(1) Risinger, A.L.; Giles, F.J.; Mooberry, S.L. Microtubule Dynamics as a target in Oncology . *Cancer Treat. Rev.* **2009**, *35*, 255-261.

(2) Desai, A.; Mitchison, T.J. Microtubule Polymerization dynamics. *Annu. Rev. Cell Dev. Biol*. **1997**, *13*, 83-117.

(3) Jordan, M.; Wilson, L. Microtubules as a Target for Anticancer Drugs. *Nat. Rev. Cancer* **2004**, *4*, 253-65.

(4) Rowinsky, E.K.; Calvo E. Novel Agents that Target Tubulin and Related Elements. *Semin. Oncol.* **2006**, *33*, 421-435.

(5) Yue, Q.X.; Liu, X.; Guo, D.A. Microtubule-Binding Natural Products for Cancer Therapy. *Planta Med.* **2010**, *11*, 1037-1043.

(6) Gupta, S.; Bhattacharyya, B. Antimicrotubular Drugs Binding to Vinca Domain of Tubulin. *Mol. Cell Biochem*. **2003**, *253*, 41-47.

(7) Hinnen, P.; Eskens, F.A.L.M. Vascular Disrupting Agents in Clinical Development. *Br. J. Cancer* **2007**, *96*, 1159-1165.

(8) Roberti, M.; Pizzirani, D.; Simoni, D.; Rondanin, R.; Barucchello, R.; Bonora, C.; Buscemi, F.; Grimaudo, S.; Tolomeo, M. Synthesis and Biological Evaluation of Resveratrol and Analogues as Apoptosis-Inducing Agents. *J. Med. Chem.* **2003**, *46*, 3546-3554.

(9) Bai, R.; Durso, N.A.; Sackett, D.L.; Hamel, E. Interactions of the Sponge-Derived Antimitotic Tripeptide Hemiasterlin with Tubulin: Comparison with Dolastatin 10 and Cryptophycin 1. *Biochemistry* **1999**, *38*, 14302–14310.

(10) Loganzo, F.; Discafani, C.M.; Annable, T.; Beyer, C.; Musto, S.; Hari, M.; Tan, X.; Hardy, C.; Hernandez, R.; Baxter, M.; Singanallore, T.; Khafizova, G.; Poruchynsky, M.S.; Fojo, T.; Nieman, J.A., Ayral-Kaloustian, S.; Zask, A.; Andersen, R.J.; Greenberger, L.M. HTI-286, a Synthetic Analogue of the Tripeptide Hemiasterlin, is a Potent Antimicrotubule Agent that

Circumvents P-Glycoprotein-Mediated Resistance in Vitro and in Vivo. *Cancer Res.* **2003**, *63*, 1838–1845.

(11) Nieman, J.A.; Coleman J.E.; Wallace D.J.; Piers, E.; Lim, L.Y.; Roberge, M.; Andersen, R.J. Synthesis and Antimitotic/Cytotoxic Activity of Hemiasterlin Analogues. *J. Nat. Prod.* **2003**, *66*, 183–199.

(12) Zask, A.; Kaplan, J.; Musto, S.; Loganzo, F. Hybrids of the Hemiasterlin Analogue Taltobulin and the Dolastatins are Potent Antimicrotubule Agents. *J. Am. Chem. Soc*. **2005**, *127*, 17667-17671.

(13) Simoni, D.; Lee, R.M.; Durrant, D.E.; Chi, N.W.; Baruchello, R.; Rondanin, R.; Rullo, C., Marchetti, P. Versatile Synthesis of New cytotoxic Agents Structurally related to Hemiasterlins. *Bioorg. Med. Chem. Lett.* **2010**, *20*,3431-3435.

(14) Hsu, L.C., Durrant, D.E., Huang, C.C.; Chi, N.W.; Baruchello, R.; Rondanin, R.; Rullo, C.; Marchetti, P.; Grisolia, G.; Simoni, D.; Lee, R.M. Development of Hemiasterlin Derivatives as Potential Anticancer Agents that Inhibit Tubulin Polymerization and Synergize with a Stilbene Tubulin Inhibitor. *Invest. New Drugs* **2012**, *30*, 1379-1388.

(15) Simoni, D.; Invidiata, F.P.; Eleopra, M.; Marchetti, P.; Rondanin, R.; Baruchello, R.; Grisolia, G.; Tripathi, A.; Kellogg, G.E.; Durrant, D.; Lee, R.M. Design, Synthesis and Biological Evaluation of Novel Stilbene-Based Antitumor Agents. *Bioorg. Med. Chem.* **2009**, *17,* 512-522.

(16) Lowry, O. H.; Rosebrough, N. J.; Farr, A. L.; Randall, R. J. Protein Measurement with the Folin Phenol Reagent. *J. Biol. Chem.* **1951**, *193*, 265−275.

(17) Dalpiaz, A.; Paganetto, G.; Pavan, B.; Fogagnolo, M.; Medici, A.; Beggiato, S.; Perrone, D. Zidovudine and Ursodeoxycholic Acid Conjugation: Design of a New Prodrug Potentially Able to Bypass the Active Efflux Transport Systems of the Central Nervous System. *Mol. Pharm*. **2012**, *9*, 957-968.

(18) Artursson, P.; Karlson, J. Correlation between Oral Absorption in Humans and Apparent Drug Permeability Coefficients in Human Intestinal Epithelial (Caco-2) Cells. *Biochem. Biophys. Res. Commun.* **1991**, *175*, 880-885.

(19) Pal, D.; Udata, C.; Mitra, A. K. Transport of Cosalane, a Highly Lipophilic Novel Anti-HIV Agent, across Caco-2 Cell Monolayers. *J. Pharm. Sci.* **2000**, *89*, 826-833.

(20) Raje, S.; Cao, J.; Newman, A. H.; Gao, H.; Eddington, N. D. Evaluation of the Blood-Brain Barrier Transport, Population Pharmacokinetics, and Brain Distribution of Benztropineanalogs and Cocaine Using in Vitro and in Vivo Techniques. *J. Pharmacol. Exp. Ther.* **2003**, *307*, 801-808.

(21) Yee, S. In Vitro Permeability across Caco-2 Cells (Colonic) Can Predict in Vivo (Small Intestine) Absorption in Man - Fact or Myth. *Pharm. Res.* **1997**, *14*, 763-766.

(22) *a)* D'angeli, F.; Marchetti, P.; Bertolasi V. Stereoselective Substitution in 2-Bromo Amides in the Presence of Ag^{+} or Ag_2O. *J. Org. Chem,* **1995**, *60*, 4013-4016. *b)* Marchetti, P.; D'Angeli, F.; Bertolasi, V. Stereoselective Synthesis of Neutral and Cationic 2-Heterocyclically Substituted Propanamides. *Tetrahedron: Asymmetry* **1997**, *8*, 3837-3842. *c)* Maran, F. Electrochemical and Stereochemical Investigation on the Mechanism of the Decay of 2-Halo Amide Anions. The Intermediacy of Aziridinones. *J. Am. Chem. Soc.* **1993***, 115*, 6557-6563.

(23) Pavan, B.; Paganetto, G.; Rossi, D.; Dalpiaz A. Multidrug Resistance in Cancer or Inefficacy of Neuroactive Agents: Innovative Strategies to Inhibit or Circumvent the Active Efflux Transporters Selectively. *Drug Discov. Today* **2014**, *19*, 1563-1571.

(24) Karlsson, J.; Kuo, S.M.; Ziemniak, J.; Artursson, P. Transport of Celiprolol across Human Intestinal Epithelial (Caco-2) Cells: Mediation of Secretion by Multiple Transporters Including P-glycoprotein. *Br. J. Pharmacol.* **1993**, *110*, 1009-1016.

(25) Pavan, B.; Dalpiaz, A. Prodrugs and Endogenous Transporters: Are They Suitable for Drug Targeting into the Central Nervous System? *Curr. Pharm. Des.* **2011**, *17*, 3560-3576.

(26) Kuznetsov, G.; TenDyke, K.; Towle, M.J.; Cheng, H.; Liu J, Marsh, J.P.; Schiller, S.E.; Spyvee, M.R.; Yang, H.; Seletsky, B.M.; Shaffer, C.J.; Marceau, V.; Yao, Y.; Suh, E.M.; Campagna, S.; Fang, F.G.; Kowalczyk, J.J.; Littlefield, B.A. Tubulin-Based Antimitotic Mechanism of E7974, a Novel Analogue of the Marine Sponge Natural Product Hemiasterlin. *Mol. Cancer Ther.* **2009**, *8*, 2852–2860.

(27) Nunes, M.; Kaplan, J.; Wooters, J.; Hari, M.; Minnick, A.A. Jr; May, M.K.; Shi, C.; Musto, S.; Beyer, C.; Krishnamurthy, G.; Qiu, Y.; Loganzo, F.; Ayral-Kaloustian, S.; Zask, A.; Greenberger, L.M. Two Photo Affinity Analogues of Tripeptide, Hemiasterlin, Exclusively Label Alpha-Tubulin. *Biochemistry* **2005**, *44*, 6844–6857.

(28) Ravi, M.; Zask, A.; Rush, T.S. 3rd Structure-Based Identification of the Binding Site for the Hemiasterlin Analogue HTI-286 on Tubulin. *Biochemistry* **2005***, 44*, 15871–15879.

(29) Dalpiaz, A.; Cacciari, B.; Vicentini, C.B.; Bortolotti, F.; Spalluto, G.; Federico, S.; Pavan, B.; Vincenzi, F.; Borea, P.A.; Varani, K. A Novel Conjugated Agent between Dopamine and an A_{2A} Adenosine Receptor Antagonist as a Potential Anti-Parkinson Multitarget Approach. *Mol. Pharm*. **2012**, *9*, 591-604, 2012.

(30) Manfredini, S.; Pavan., B.; Vertuani, S.; Scaglianti, M.; Compagnone, D.; Biondi, C.; Scatturin, A.; Tanganelli, S.; Ferraro, L.; Prasad, P.; Dalpiaz, A. - Design, Synthesis and Activity of Ascorbic Acid Prodrugs of Nipecotic, Kinurenic and Diclophenamic Acids, Liable to Increase Neurotropic Activity. *J. Med. Chem.***2002**, *45***,** 559-562.

(31) Dalpiaz, A.; Pavan, B.; Scaglianti, M., Vitali, F.; Bortolotti, F.; Biondi, C.; Scatturin, A.; Tanganelli, S.; Ferraro, L.; Prasad, P.; Manfredini, S. Transporter-Mediated Effects of Diclofenamic Acid and its Ascorbyl Pro-drug in the in Vivo Neurotropic Activity of Ascorbyl Nipecotic Acid Conjugate. *J. Pharm. Sci.* **2004**, *93,* 78-85.

(32) Dalpiaz, A.; Pavan, B.; Scaglianti, M.; Vitali, F.; Bortolotti, F.; Biondi, C.; Scatturin, A.; Manfredini, S. Vitamin C and 6-Amino-vitamin C Conjugates of Diclofenac: Sysnthesis and Evaluation. *Int. J. Pharm.* **2005**, *291*, 171-181.

(33) Dalpiaz, A.; Pavan, B.; Vertuani, S.; Vitali, F.; Scaglianti, M.; Bortolotti, F.; Biondi, C.; Scatturin, A.; Tanganelli, S.; Ferraro, L.; Marzola, G.; Prasad, P.; Manfredini, S. Ascorbic and 6-Br-Ascorbic Acid Conjugates as a tool to Increase the therapeutic Effects of Potentially Central Active Drugs. *Eur. J. Pharm. Sci.* **2005**, *24*, 259-269.

(34) Dalpiaz, A.; Filosa, R.; de Caprariis, P.; Conte, G.; Bortolotti, F.; Biondi, C.; Scatturin, A.; Prasad P.D.; Pavan, B. Molecular Mechanism Involved in the Transport of a Prodrug Dopamine Glycosyl Conjugate. *Int. J. Pharm.* **2007**, *336*: 133-139.

(35) Dalpiaz , A.; Contado, C.; Mari, L.; Perrone, D.; Pavan, B.; Paganetto, G.; Hanuskovà, M.; Vighi, E.; Leo, E. Development and Characterization of PLGA Nanoparticles as Delivery Systems of a Prodrug of Zidovudine obtained by its Conjugation with Ursodeoxycholic Acid. *Drug Deliv.* **2014**, *21*, 221-32.

(36) Dalpiaz, A.; Ferraro, L.; Perrone, D.; Leo, E.; Iannuccelli, V.; Pavan, B.; Paganetto, G.; Beggiato, S.; Scalia, S. Brain Uptake of a Zidovudine Prodrug after nasal Administration of Solid Lipid Microparticles. *Mol. Pharm.* **2014**, *11*, 1550-1561.

(37) Breen, E.C.; Walsh, J.J. Tubulin-Targeting Agents in Hybrid Drugs. *Curr. Med. Chem.* **2010**, *17*, 609-639.

(38) Liu, Q.; Cheng, S.; Li Z, Xu, K.; Chen, G.Q. Characterization, Biodegradability and Blood Compatibility of Poly[(R)-3-hydroxybutyrate] based poly(ester-urethane)s. *J. Biomed. Mater. Res. A.* **2009,** *90*, 1162-1176.

(39) Kawashima, Y.; Yamamoto, H.; Takeuchi, H.; Hino, T.; Niwa, T. Properties of a Peptide Containing dl-lactide/glycolide Copolymer Nanospheres Prepared by Novel Emulsion Solvent Diffusion Method. *Eur. J. Pharm. Biopharm.* **1998**, 45, 41-48.

(40) Govender, T.; Riley, T.; Ehtezazi, T.; Garnett, M.C.; Stolnik, S.; Illum, L.; Davis, S.S. Defining the Drug Incorporation Properties of PLA–PEG Nanoparticles. *Int. J. Pharm.* **2000**, *199* 95–110.

(41) Govender, T.; Riley, T.; Stolnik, S.; Garnett, M.C.; Illum, L.; Davis, S.S. PLA–PEG Nanoparticles for Site Specific Delivery: Drug Incorporation Study, *J. Contr. Rel.* **2000**, 64, 318-319.

(42) Dalpiaz, A.; Leo, E.; Vitali, F.; Pavan, B.; Scatturin, A.; Bortolotti, F.; Manfredini, S., Durini, E.; Forni, F.; Brina, B.; Vandelli, M.A. Development and Characterization of Biodegradable Nanoparticles as delivery Systems of Antiischemic Adenosine Derivatives. *Biomaterials* **2005**, *26*, 1299-1306.

(43) Hu, C.M.J.; Zhang, L. Nanoparticle-Based Combination Therapy Toward Overcoming Drug Resistance in Cancer. *Biochem. Pharmacol.* **2012**, *83*, 1104–1111.

(44) Valerii, M.C.; Ricci, C.; Spisni, E.; Di Silvestro, R.; De Fazio, L.; Cavazza, E.; Lanzini, A.; Campieri, M.; Dalpiaz, A.; Pavan, B.; Volta, U.; Dinelli. G. Responses of Peripheral Blood Mononucleated Cells from non-Celiac Gluten Sensitive Patients to Various Cereal Sources. *Food Chem.* **2015,** *176*:167-174.

(45) Ferretti, V.; Dalpiaz, A.; Bertolasi, V.; Ferraro, L.; Beggiato, S.; Spizzo, F.; Spisni, E.; Pavan, B. Indomethacin Co-Crystals and their Parent Mixtures: does the Intestinal Barrier Recognize them Differently? *Mol. Pharm.* **2015**; *12*:1501-1511.

Scheme 1. Synthesis of compound **A-L**[a]

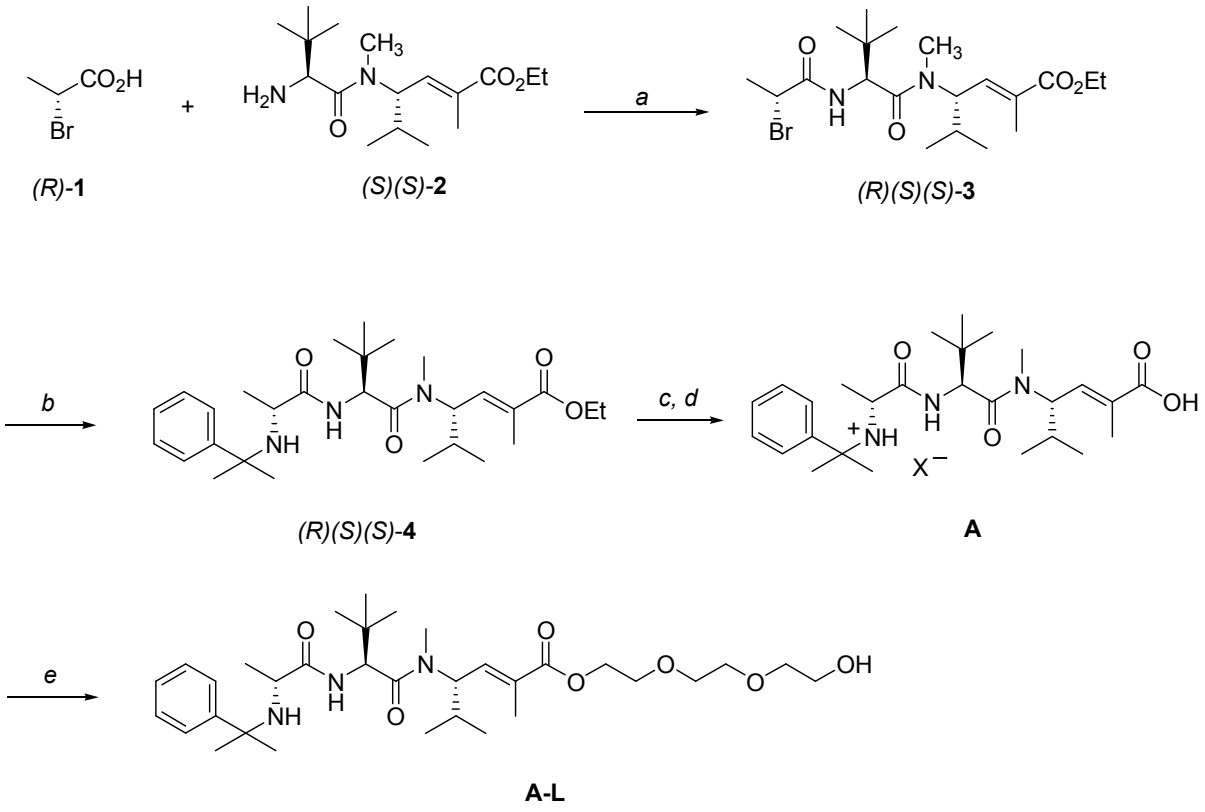

[a]Reagent and conditions: (a) PyBOP, DIEA, CH_2Cl_2, 2h, 76% (b) $PhC(CH_3)_2NH_2$, Ag_2O, Toluene, 1.5h, sonication, 90% ; (c) LiOH, $MeOH/H_2O$, 3h, 82%; (d) H^+; (e) TEG, PyBop, DIEA, CH_2Cl_2, 24h, 89%.

Scheme 2. Synthesis of the compound **A-L-B**[a]

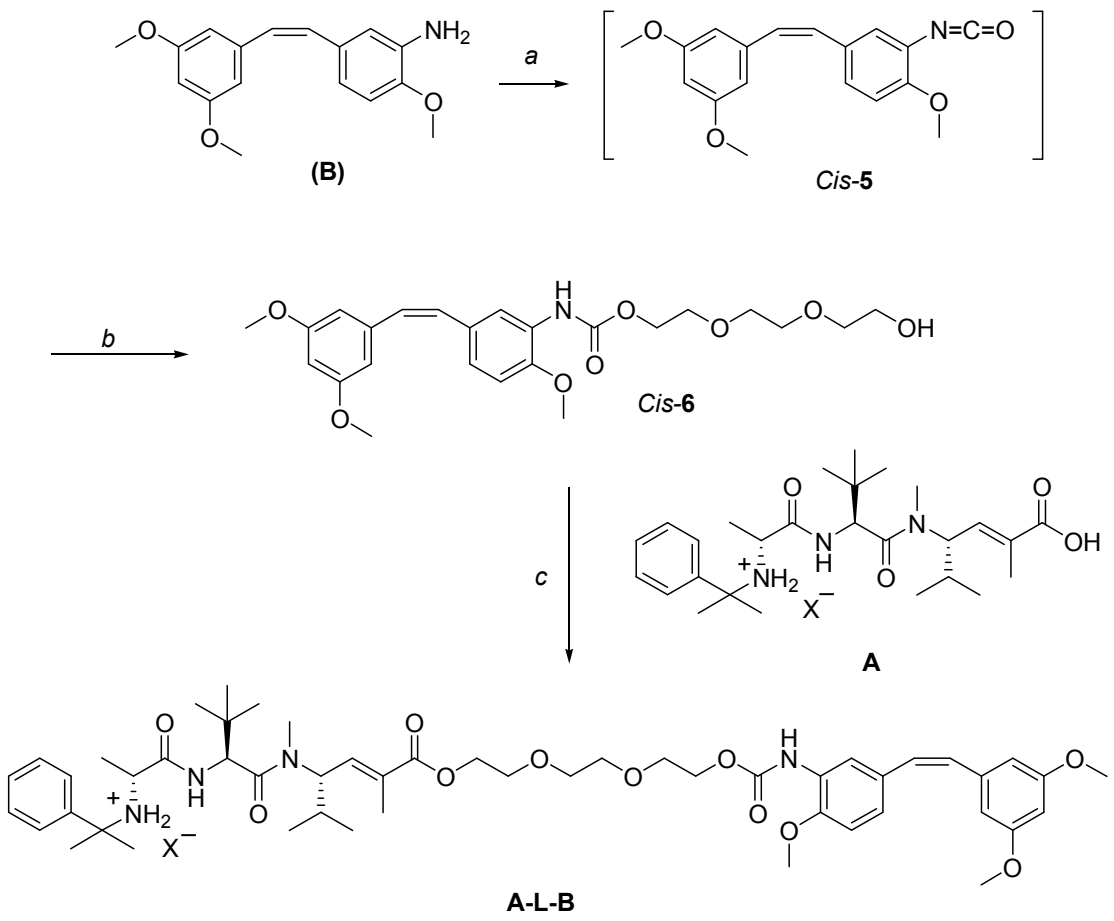

[a] Reagent and conditions: (a) Trichloromethyl chloroformate, dioxane, 60°C, 3h; (b) Triethylene glycol, dioxane, 48h, 78%, (c) PyBop, DIEA, CH_2Cl_2, 24h, 69%

Table 1. Permeability Coefficients (P_E) (×10−5 cm/min) of ***Celiprolol***, ***Taltobulin*** and Compound ***A*** Transported by the Monolayer Obtained by NCM460 Cells on Millicell System.[a] The Ratio between the P_E Values Referred to the Basolateral (B) → Apical (A) and B → A Passages are also Reported.

Compound	A → B	B → A	Ratio (B → A) /(A → B)
Celiprolol	2.95 ± 0.06	9.98 ± 0.56[b]	3.4 ± 0.2
Taltobulin	6.21 ± 0.28	6.96 ± 0.24	1.12 ± 0.06[d]
Compound A	5.28 ± 0.44	7.96 ± 0.37[c]	1.5 ± 0.1[d,e]

[a]The values were obtained from Pt and Pf coefficients according to eq 2. The coefficients are referred to the transport from the apical compartment (A) to the basolateral compartment (B) and vice versa. [b]$p < 0.001$ as compared to P_E value of ***celiprolol*** transported from A to B. [c]$p < 0.01$ as compared to P_E value of ***compound A*** transported from A to B. [d]$p < 0.001$ as compared to ratio value of ***celiprolol***. [e]$p > 0.05$ as compared to ratio value of ***taltobulin***.

Caption of Figures

Figure 1. Chemical formulas of the hemiasterlin (***A***, ***A-L***), stilbene (***B***, ***B-L***) derivatives and their hybrid ***A-L-B*** analyzed. The stilbene derivative ***C*** was employed as internal standard for HPLC analysis. $X^- = CF_3CO_2^-$

Figure 2. [a] Degradation profiles of the compounds ***A***, ***A-L***, ***B***, ***B-L*** and hybrid ***A-L-B*** in rat whole blood. All the values are reported as the percentage of the overall amount of incubated prodrug. [b] Semi logarithmic plots of the degradation profiles; their linearity ($n = 9$, $r \geq 0.990$, $P < 0.0001$) evidences a degradation following an apparent first order kinetic (half-lives = 25.4 ± 1.1 min for ***A-L***, 288 ± 12 min for ***B-L*** and 118.2 ± 9.5 min for ***A-L-B***). No degradation was detected for compounds **A** and **B**. Data are reported as the mean ± SD of three independent experiments.

Figure 3. Degradation profiles of the compounds ***A-L*** (a), ***B-L*** (b) and ***A-L-B*** (c) with the corresponding appearance profiles of their hydrolysis products in rat whole blood. All the values are reported as the percentage of the overall amount of incubated compounds and as the mean ± SD of three independent experiments.

Figure 4. [a] Degradation profiles of the compounds ***A***, ***A-L***, ***B***, ***B-L*** and hybrid ***A-L-B*** in rat liver homogenates. All the values are reported as the percentage of the overall amount of incubated prodrug. [b] Semi logarithmic plots of the degradation profiles; their linearity ($n = 9$, $r \geq 0.973$, $P < 0.0001$) evidences a degradation following an apparent first order kinetic (half-life of ***A-L*** =118.0 ± 7.2 min). The degradations of compounds ***B-L*** and hybrid ***A-L-B*** were less than 30% during eight hours of incubation. No degradation was detected for compounds **A** and **B**. Data are reported as the mean ± SD of three independent experiments.

Figure 5. Degradation profiles of the compounds ***A-L*** (a), ***B-L*** (b) and ***A-L-B*** (c) with the corresponding appearance profiles of their hydrolysis products in rat liver homogenates. All the values are reported as the percentage of the overall amount of incubated compounds and as the mean ± SD of three independent experiments.

Figure 6. Expression of multi-drug resistance channel genes in NCM460 cells. The RNA isolated from NCM460 cells was retro transcribed and the cDNAs were amplified by couples of primers specific for the beta-actin (lane 1), ABCB1 (lane 2) or ABCC1 (lane 3) genes. As negative control the un-reverted RNA was amplified in the presence of primers specific for ABCB1 (lane 4) and ABCC1 (lane 5). Electrophoresis on 1% agarose gel showed PCR products of the expected size. M = pUC mix marker 8 (Fermentas)**.**

Figure 7. Permeation kinetics of ***taltobulin*** [a], ***celiprolol*** [b] and compound ***A*** [c] across the Millicell filters alone or coated by monolayers obtained by NCM460 cells (filters with cells). The permeations were analyzed from the apical to basolateral compartments (A → B) [a] and from the basolateral to apical compartments (B → A) [b]. The cumulative amounts in the receiving basolateral compartment were linear within 120 min or 150 min ($r \geq 0.995$, $P \leq 0.002$) in all cases analyzed. All data are reported as mean ± SD of three independent experiments.

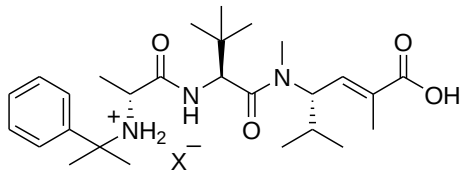

A

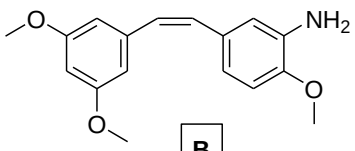

B

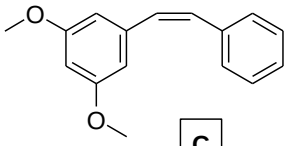

C

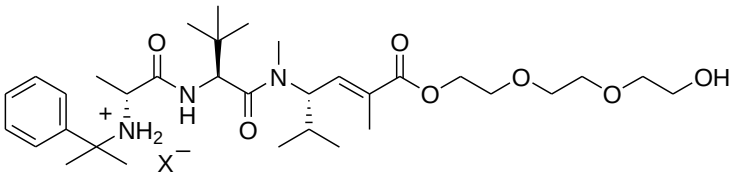

A-L

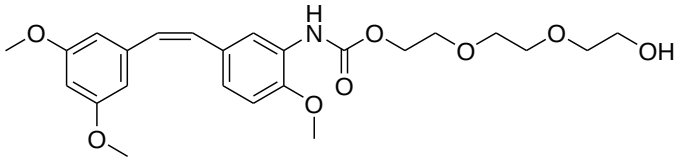

B-L

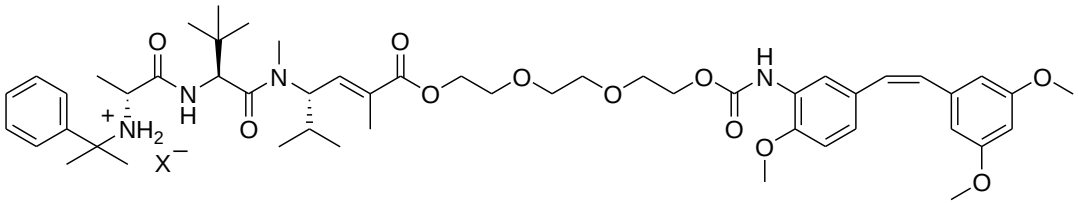

A-L-B

Figure 1

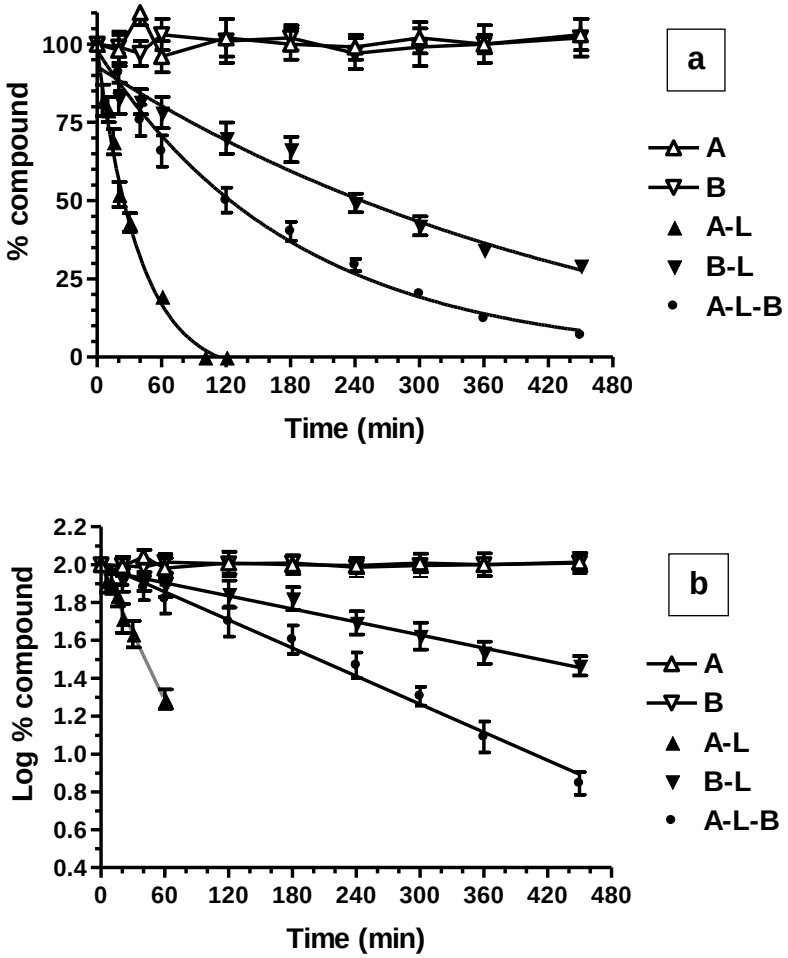
a
% compound
100
75
50
25
0
0 60 120 180 240 300 360 420 480
Time (min)
A
B
A-L
B-L
A-L-B
b
Log % compound
2.2
2.0
1.8
1.6
1.4
1.2
1.0
0.8
0.6
0.4
0 60 120 180 240 300 360 420 480
Time (min)
A
B
A-L
B-L
A-L-B

Figure 2

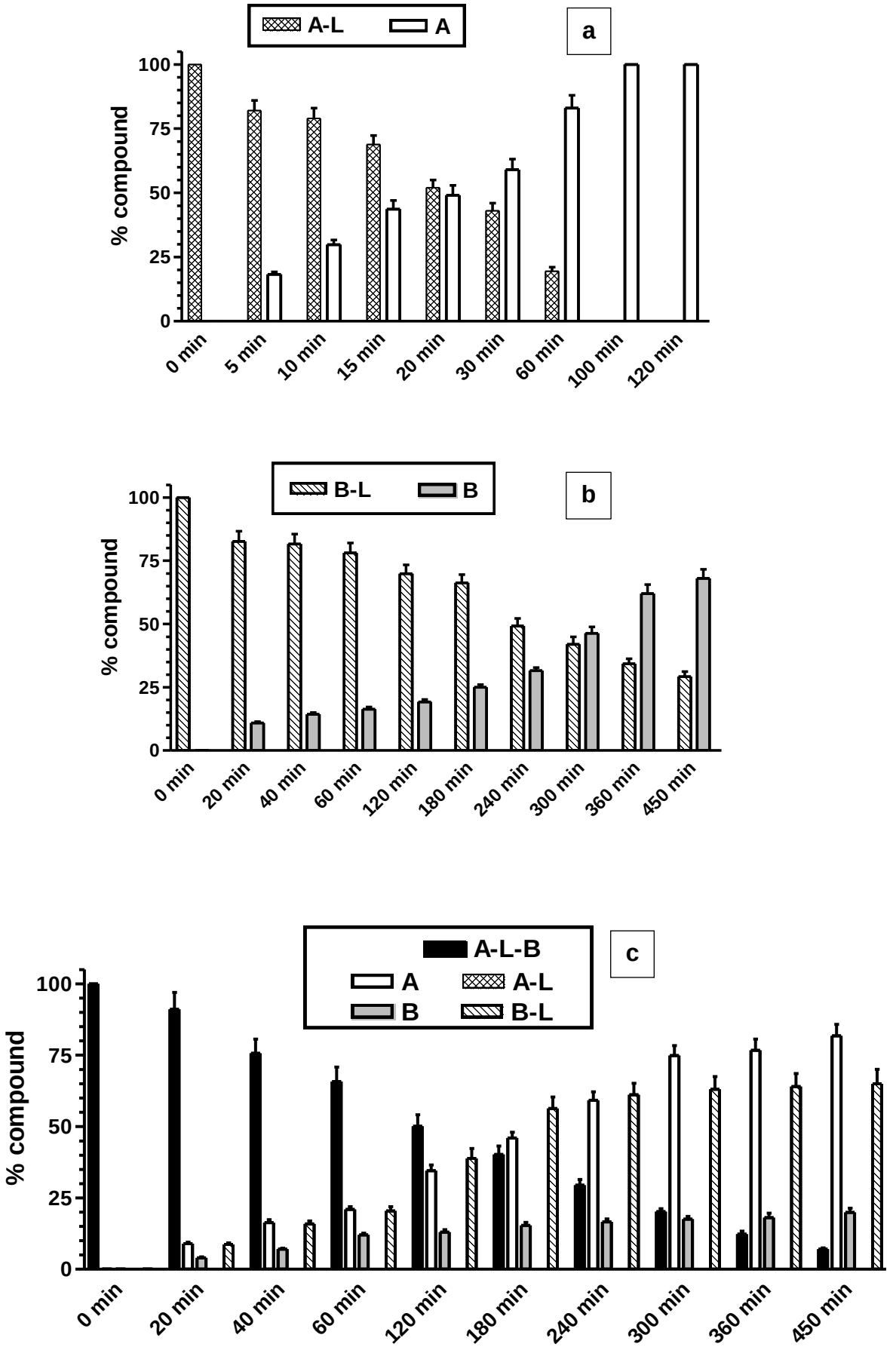
A-L
A
a
% compound
100
75
50
25
0
0 min
5 min
10 min
15 min
20 min
30 min
60 min
100 min
120 min
B-L
B
b
% compound
100
75
50
25
0
0 min
20 min
40 min
60 min
120 min
180 min
240 min
300 min
360 min
450 min
A-L-B
A
A-L
B
B-L
c
% compound
100
75
50
25
0
0 min
20 min
40 min
60 min
120 min
180 min
240 min
300 min
360 min
450 min

Figure 3

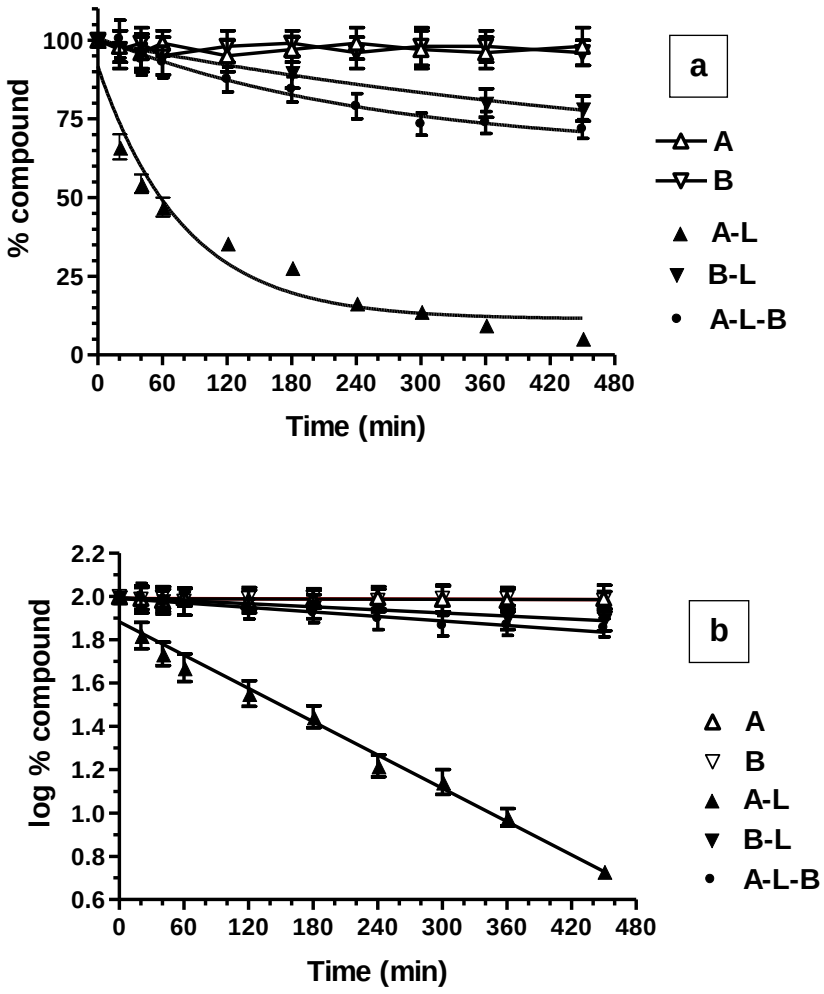
a
% compound
100
75
50
25
0
0 60 120 180 240 300 360 420 480
Time (min)
A
B
A-L
B-L
A-L-B
b
log % compound
2.2
2.0
1.8
1.6
1.4
1.2
1.0
0.8
0.6
0 60 120 180 240 300 360 420 480
Time (min)
A
B
A-L
B-L
A-L-B

Figure 4

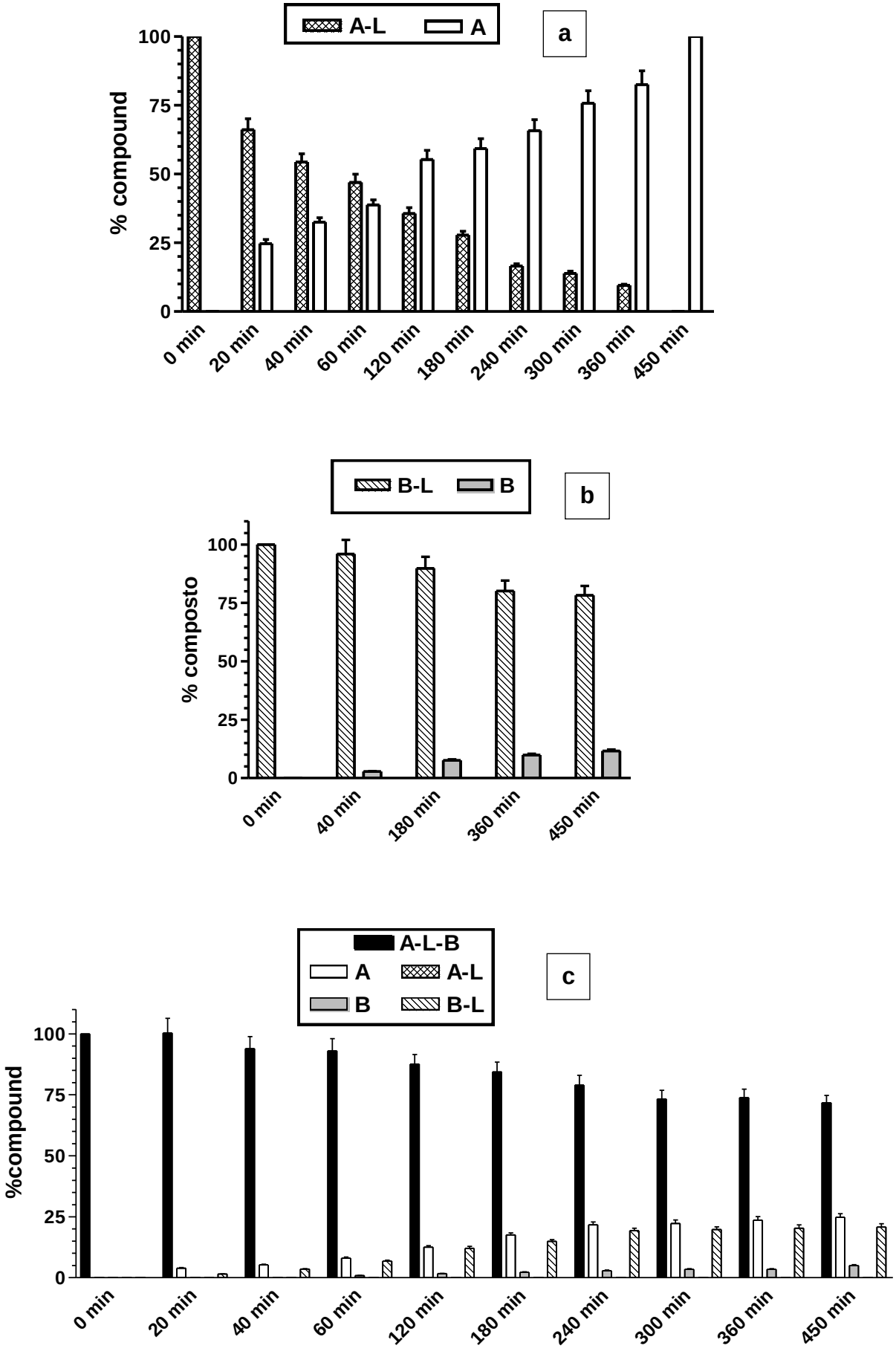
A-L
A
a
% compound
100
75
50
25
0
0 min
20 min
40 min
60 min
120 min
180 min
240 min
300 min
360 min
450 min
B-L
B
b
% composto
100
75
50
25
0
0 min
40 min
180 min
360 min
450 min
A-L-B
A
A-L
B
B-L
c
%compound
100
75
50
25
0
0 min
20 min
40 min
60 min
120 min
180 min
240 min
300 min
360 min
450 min

Figure 5

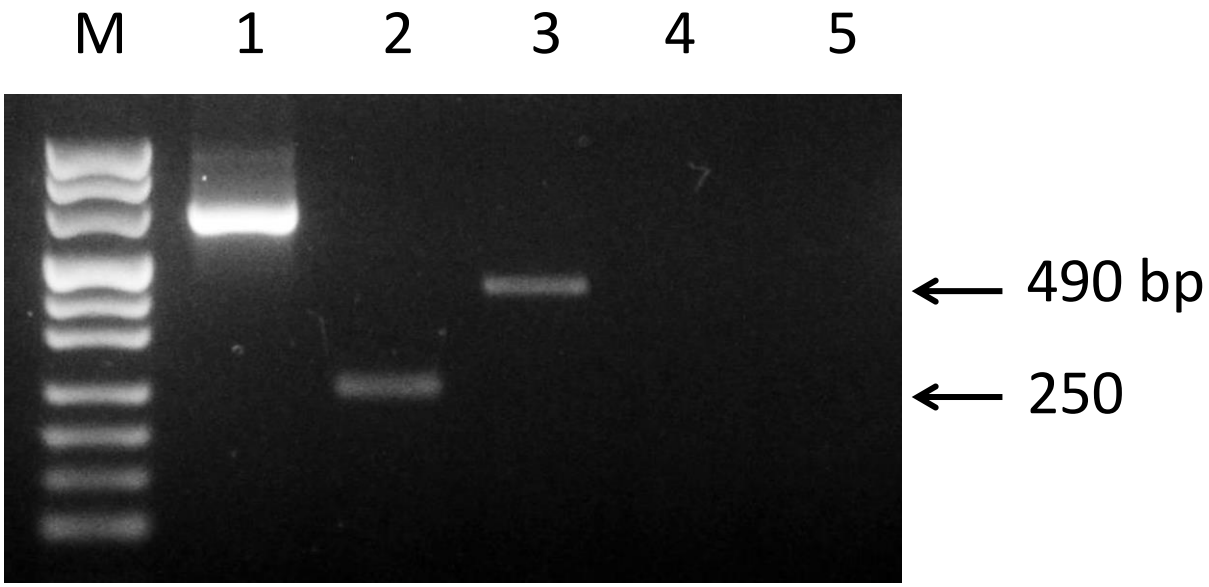

Figure 6

a

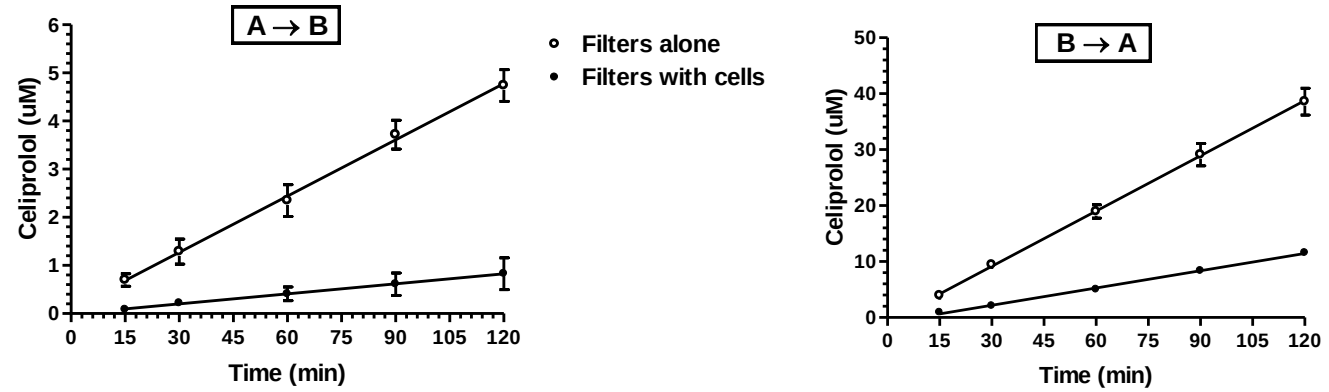
A → B
Celiprolol (uM)
Time (min)
Filters alone
Filters with cells
B → A
Celiprolol (uM)
Time (min)

b

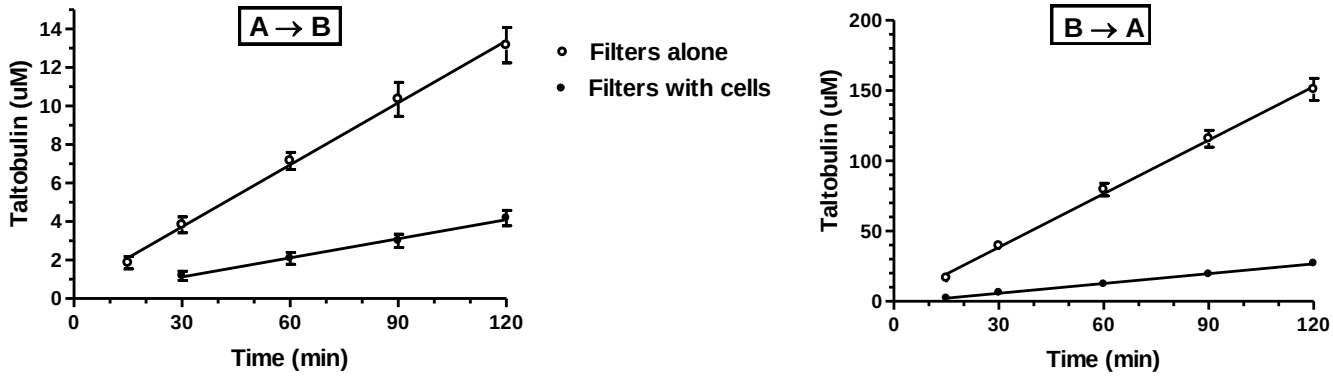
A → B
Taltobulin (uM)
Time (min)
Filters alone
Filters with cells
B → A
Taltobulin (uM)
Time (min)

c

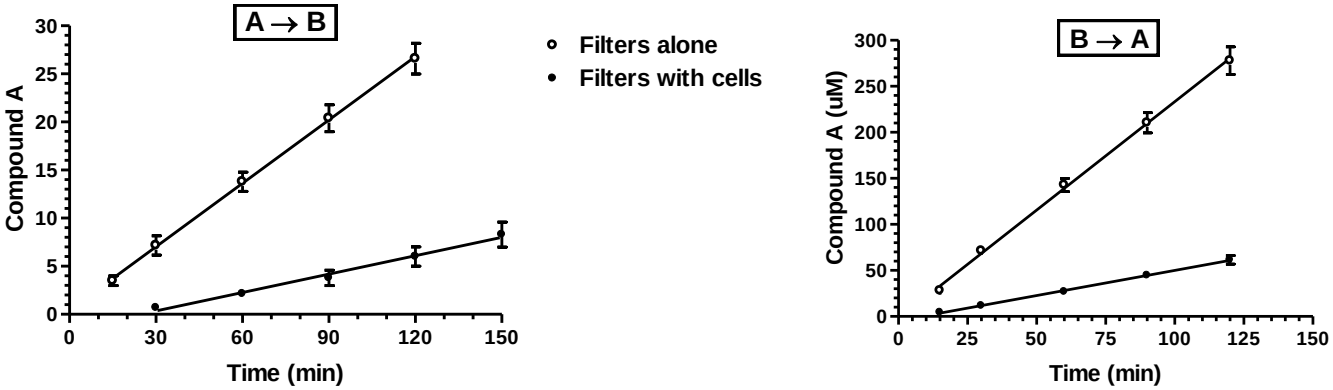
A → B
Compound A
Time (min)
Filters alone
Filters with cells
B → A
Compound A (uM)
Time (min)

Figure 7